Universidade de Lisboa

Faculdade de Ciências

Departamento de Biologia Vegetal

Deciphering the role of inflammation in the organotypic hippocampal slice model of epileptogenesis

Daniela Cristina Melo Magalhães

Dissertação

Mestrado Biologia Molecular e Genética

2015

Universidade de Lisboa

Faculdade de Ciências

Departamento de Biologia Vegetal

Deciphering the role of inflammation in the organotypic hippocampal slice model of epileptogenesis

Daniela Cristina Melo Magalhães

Dissertação

Mestrado Biologia Molecular e Genética

Orientadores

Prof. Doutor Rui Gomes, Faculdade de Ciências da Universidade de Lisboa
Doutora Cláudia Valente de Castro, Instituto de Medicina Molecular, Lisboa

2015

Acknowledgements

Gostaria de agradecer à Doutora Cláudia Valente pelo seu enorme apoio e acessibilidade ao longo de todo o trabalho e por todos os ensinamentos transmitidos, que me foram muito valiosos para sua concretização. Por fim gostaria também de agradecer a sua amizade e paciência durante este último ano e meio.

Ao professor Alexandre Ribeiro e à professora Ana Sebastião por terem concedido a oportunidade de realizar o meu estágio de mestrado na área das Neurociências e por todos os conselhos dados.

Ao Professor Rui Gomes pela disponibilidade cedida sempre no esclarecimento de todos os assuntos legislativos e pela ajuda no laboratório.

Gostaria também de agradecer à Noémia Pereira que sempre me ajudou desde o primeiro dia de estágio e à Rita Aroeira pela disponibilidade constante e pelos seus preciosos conselhos. A elas agradeço todo o seu apoio.

À Cláudia Cavacas pela sua ajuda nos últimos meses e por *cuidar* das minhas culturas sempre que era preciso e claro, pela sua amizade, apoio e muita paciência tanto nos melhores momentos como nos menos bons.

A todos os restantes colegas de laboratório que me ajudaram e motivaram durante a realização da tese.

Ao Carlos Posse e à Vera Salgado pela motivação e pela disponibilidade de ouvirem os meus desabafos.

Por fim, deixo um agradecimento especial aos meus pais por me proporcionarem a oportunidade de realizar o estágio e por todos os conselhos e apoio incondicional.

Resumo

A epilepsia é uma das mais prevalentes desordens neurológicas em todo o mundo, afetando 0.4-1% da população mundial. De acordo com dados da Organização Mundial de Saúde a epilepsia é responsável por 1% dos encargos com doenças. O termo epilepsia inclui várias desordens neurológicas genéticas e adquiridas que têm em comum a ocorrência periódica e imprevisível de convulsões, isto é, de episódios de atividade neuronal excessiva. Embora estejam disponíveis vários fármacos antiepilépticos, estes não são eficazes em 30% dos pacientes que continuam a sofrer progressão da doença. Torna-se então imperativo encontrar novas terapias que previnam o início e/ou progressão desta desordem.

Tradicionalmente a epilepsia tem sido considerada unicamente como uma doença neuronal. No entanto, na última década, vários estudos realizados em modelos animais de epilepsia e em tecido cerebral humano de pacientes com esta desordem demonstraram a influência e a contribuição de processos inflamatórios nos mecanismos de geração e recorrência dos ataques epiléticos. A neuroinflamação pode ser vista como uma resposta imune que têm como objetivo enfrentar uma ameaça que esteja a ocorrer no cérebro. No entanto, a inflamação pode ser tanto prejudicial como benéfica na resolução da lesão. Vários estudos demonstraram que um processo inflamatório ocorre em todos os tipos de epilepsia, mesmo nos tipos sem características da fisiopatologia inflamatória, tal como epilepsia do lobo temporal (TLE). TLE é um dos principais e mais perigosos tipos de epilepsia que afeta a zona do hipocampo. Estudos recentes mostraram que o estado de inflamação crónica nesta doença está de facto associado à morte neuronal, à ativação de células da glia e à expressão de fatores inflamatórios. As células da glia, nomeadamente astrócitos e microglia, têm um papel relevante na inflamação através da sobrexpressão e libertação de mediadores inflamatórios, tais como as citocinas. Estas proteínas possuem efeitos tanto na disfunção sináptica como na excitoxicidade e na morte neuronal que podem contribuir para a alteração da excitabilidade neuronal, levando à epileptogénese. As principais citocinas pro-inflamatórias envolvidas na geração e propagação das convulsões são o factor de necrose tumoral (TNF-α), a interleucina-1β (IL-1β) e a interleucina-6 (IL-6).

Este estudo pretende avaliar a evolução dos eventos inflamatórios num modelo *in vitro* de epileptogénese. O estudo foca-se na morte celular, no estado de activação e morfologia dos astrócitos e da microglia, assim como na expressão das principais citocinas pro-inflamatórias envolvidas na epilepsia.

Para realizar estes objetivos foram usadas culturas organotípicas de hipocampo, uma vez que, recentemente foi descrita a ocorrência de atividade epilética espontânea nestas culturas. Estas culturas são extremamente atrativas uma vez que as células se desenvolvem de forma semelhante às células *in vivo*, e podem ser mantidas por longos períodos de tempo permitindo uma manipulação e avaliação a longo prazo. O processo de corte do hipocampo para obtenção das fatias organotípicas representa um trauma bastante severo com o consequente desenvolvimento de conectividade anormal, que também se encontra descrito em tecido humano de pacientes com epilepsia. Por estes motivos, as culturas organotípicas de hipocampo são consideradas um modelo simples e útil no estudo da epileptogénese. As culturas foram preparadas a partir de ratos Sprague-Dawley com 6-7 dias de vida (P6-7). Todos os ensaios foram realizados em amostras obtidas a 7, 14 e 21 dias *in vitro* (DIV), de modo a estudar a morte celular e os marcadores de inflamação ao longo do tempo.

A morte celular foi avaliada através da captação de iodeto de propídio (PI) e dos produtos de clivagem da α-II Espectrina (SBDP). O PI é um marcador fluorescente com a capacidade de se ligar aos ácidos nucléicos. Deste modo, ao entrar nas células cujas membranas estão danificadas (ou seja, em processo de morte celular) permite observá-las num microscópio de fluorescência. Os SBDP dão indicação sobre o tipo de morte celular que está a ocorrer nas células, uma vez que α-II Espectrina pode ser clivada por protéases envolvidas na morte celular, nomeadamente a calpaína (ativada tanto na necrose como na apoptose) e a caspase-3 (principal caspase ativada na apoptose), dando origem a produtos distintos. A ativação dos astrócitos e da microglia foi analisada por western blot através da expressão de marcadores específicos. Para os astrócitos utilizou-se como marcador a proteína acídica fibrilar glial (GFAP) e para a microglia a molécula de ligação ao cálcio ionizado 1 (Iba1). O ensaio de imunofluorescência, realizado com os marcadores referidos, foi efetuado para avaliar as alterações morfológicas destas células da glia, uma vez que a sua forma é indicadora do seu estado de ativação. Adicionalmente, a expressão de mRNA das citocinas, assim como dos seus receptores, foi quantificada por PCR quantitativo.

O ensaio de morte celular por PI mostrou que a região CA1 do hipocampo é a zona mais sensível, o que está de acordo com a literatura. A zona CA1 sofre uma reorganização de conexões neuronais e apresenta uma maior concentração de recetores de glutamato, cuja activação pode conduzir à morte das células. Relativamente à progressão da morte celular, tanto os resultados do PI como os SBDP demonstraram um pico de morte celular a 14 DIV. Este resultado coincide com o início de atividade epiléptica espontânea observada neste modelo e

considera-se ser uma consequência destes eventos. Neste trabalho apenas o SBDP resultante da clivagem da α-II Espectrina pela calpaína foi obtido. Não se obtive o SBDP resultante da clivagem da α-II Espectrina pela caspase-3, nem a forma ativa desta mesma caspase. Concluiu-se assim que a morte celular neste modelo ocorre por necrose ou pela via de apoptose não dependente das caspases, uma vez que a calpaína atua em ambos os tipos de morte celular.

A expressão do GFAP teve um ligeiro aumento ao longo do tempo, mas sem significado estatístico. No entanto, nas imagens de imunofluorescência pode observar-se a formação progressiva de uma cicatriz glial. Esta cicatriz é caracterizada pela presença de astrócitos com processos longos e entrelaçados a cobrir os neurónios, e tem como função restringir espacialmente a inflamação e o tecido danificado. De facto, a ocorrência de cicatriz glial generalizada, isto é, observável em todas as zonas do hipocampo, coincidiu com o pico de morte celular reportado neste estudo. O western blot indicou uma redução de cerca de 40% na expressão do marcador da microglia (Iba-1), tanto a 14 DIV como a 21 DIV, comparativamente a 7 DIV. O ensaio de imunofluorescência mostrou a ocorrência da morfologia "amoeboid", característica de microglia activada e com maior expressão de Iba1 apenas a 7 DIV, tendo posteriormente ocorrido uma reversão para a morfologia ramificada, típica de microglia não ativa.

A avaliação da expressão dos transcritos das citocinas indicou um aumento progressivo ao longo do tempo, relativamente à IL-1β e TNF-α. A IL-6 aumentou significativamente apenas a 21 DIV. A expressão da maioria dos respectivos recetores das citocinas estudadas também mostrou um aumento significativo a 21 DIV. Apenas o recetor TNFR2 do TNF-α teve um aumento estatístico significativo, o que poderá indicar um aumento de sinalização anti-apóptotica a 21 DIV, explicando a diminuição de morte celular obtida nesse tempo.

Neste modelo de epileptogénese, obteve-se uma progressão de eventos inflamatórios com aumento de gliose e de citocinas inflamatórias, coincidente com o desenvolvimento da atividade epilética espontânea. Observou-se a ocorrência de astrogliose progressiva, enquanto a microglia reverteu para um estado inativado ao longo do tempo. Neste trabalho, a ativação da microglia parece estar relacionada com a lesão infligida pelo método de preparação das fatias de hipocampo, uma vez que a microglia atua muito rapidamente em situações de lesão (e também de infeção e/ou inflamação), sendo um dos seus principais papéis eliminar os restos celulares resultantes da morte das células. A ativação da microglia é também responsável por promover a ativação dos astrócitos, que representam neste modelo a fonte principal de produção dos

mediadores inflamatórios, sendo assim responsáveis por perpetuar o estado de inflamação na epileptogénese.

Este trabalho mostrou que o modelo de epileptogénese usado é bastante útil para explorar as funções das células da glia e da inflamação na epileptogénese e na progressão da epilepsia.

Palavras-chave:
Epilepsia, Neuroinflamação, Gliose, Citocinas, Hipocampo

Abstract

Epilepsy is one of the most common neurological disorders. The influence of inflammatory processes on epilepsy has increased in the last decade and recent studies show the contribution of astrocytes and microglia for the mechanisms of seizure onset and recurrence, through the overproduction and release of pro-inflammatory cytokines.

The aim of this study was to explore the progression of inflammatory markers within the organotypic hippocampal slice model of epileptogenesis.

An evaluation of cell death was performed through Propidium Iodide uptake assay and alphaII-Spectrin cleavage. Astrogliosis and microglia activation were also assessed by western blot and by immunofluorescence assays, which used specific markers for astrocytes and microglia, glial fibrillary acidic protein (GFAP) and ionized calcium-binding molecule 1 (Iba1), respectively. Additionally, the transcript expression of the principal pro-inflammatory cytokines, involved in seizure generation and propagation (IL-1β, TNF-α and IL-6) and their receptors, was achieved through qPCR. All assays were carried out in slices with 7, 14 and 21 *days in vitro* (DIV).

The majority of cell death was obtained in 14 DIV slices, which coincided with the onset of seizure-like activity in this model. Concerning glia activation, an upregulation of GFAP, with glial scar formation, was observed throughout culture time, while microglia changed from an activated amoeboid form to a resting ramified state. Transcript analysis of all pro-inflammatory cytokines revealed an increased expression over time in culture. However, statistical significance was solely achieved in 21 DIV slices. IL-1R1, TNFR2, and IL-6R expression were also upregulated in 21 DIV slices, while TNFR1 levels remained unchanged through time in culture.

The results indicate an activity dependent inflammatory process, since at 21 DIV, when slices depict mixed interictal and ictal-like events, an upregulation of inflammatory mediators was observed in the organotypic model of epileptogenesis. More specifically, gliosis and increased expression of inflammatory mediators was achieved.

Key words:
Epilepsy, Neuroinflammation, Gliosis, Cytokines, Hippocampus

List of abbreviations

Aβ	Amyloid beta
Ab	Antibody
AEDs	Anti-epileptic drugs
AIF	Apoptosis inducing factor
AMPA	α-amino-3-hydroxy-5-methyl-4-isoxazolepropionic acid
BBB	Blood-brain-barrier
BSA	Bovine serum albumin
CA	Cornus ammonis
cDNA	Complementary DNA
CNS	Central nervous system
CP	Crossing point
Ct	Cycle threshold
DD	Death Domain
DG	Dentate gyrus
DIV	*Days in vitro*
DNA	Deoxyribonucleic acid
dNTPs	Deoxyribonucleotides thrisphosphate
dsDNA	Double-stranded DNA
DTT	Dithiothreitol
EDTA	Ethykenediamine tetraacetic
FADD	Fas-associated death domain protein
GABA	γ-Aminobutyric acid
GAPDH	Glyceraldehyde 3-phosphate dehydrogenase
GBSS	Gey's balanced salt solution
GFAP	Glial fibrillary acidic protein
gp130	Glycoprotein 130
HRP	Horseradish Peroxidase
HS	Hippocampal sclerosis

Iba1	Ionized calcium-binding molecule 1
ICE	IL-1β converting enzyme
IF	Immunofluorescense
IL-1β	Interleukin-1β
IL-1RI	IL-1 receptor type I
IL-1RII	IL-1 receptor type II
IL-1RAcP	IL-1 receptor-accessory protein
IL-6	Interleukin-6
IL-6R	IL-6 receptor
JNK	Jun N-terminal kinases
mAbs	Monoclonal antibodies
MAPKs	Mitogen-activated protein kinases
$MgCl_2$	Magnesium chloride
mTNF	Membrane TNF
MyD88	Myeloid differentiation factor 88
NF-κB	Nuclear factor-κB
NMDA	N-methyl-D-aspartate
NP40	Nonyl phenoxlpoylethano 40
OHSC	Organotypic hippocampal slice culture
PBS	Phosphate-buffer solution
PCR	Polymerase chain reaction
PFA	Paraformaldehyde
PI	Propidium iodide
PMSF	Phenylmethysulfonyl fluoride
PNS	Peripheral nervous system
PVDF	Polyvinylidene difluoride
qPCR	Quantitative real-time polymerase chain reaction
RIPA	Ristocetin induced platelet agglutination
RNA	Ribonucleic acid
RT	Reverse transcription

SBDP	Spectrin break down products
SDS	Sodium dodecyl sulfate
PAGE	Polyacrylamide gel electrophoresis
SEM	Standard error of the mean
sTNF	Soluble TNF
TACE	TNF-α converting enzyme
TAE	Tris-acetate-Ethykenediamine tetraacetic
TBS-T	Tris base solution with Tween
TLE	Temporal Lobe Epilepsy
TIM	TRAF interacting motifs
TNF-α	Tumor necrosis factor-alpha
TNFR1	TNF receptor type 1
TNFR2	TNF receptor type 2
TRADD	TNF receptor associated death domain
TRAFF	TNFR-associated factors

Index

1 BACKGROUND

1.1 Nervous System

The nervous system consists of two main parts: the central nervous system (CNS) that contains the brain and spinal cord and the peripheral nervous system (PNS) that includes the somatic and autonomic system [1]. The cellular unit of the nervous system is the neuron. However, the brain tissue is also composed by other very important cells, the glia. The neuron is an electrically excitable cell that processes and transmits information by electrical and chemical signals. Neurons are able to communicate with each other through the generation and propagation of nervous impulses and through the release of signalling molecules (the neurotransmitters), which are used to amplify and modulate signals between two neurons and also between neurons and other cells [2].

1.2 Epilepsy

Epilepsy is the third most common chronic brain disorder affecting 0,4-1% of the world's population [3,4]. The International League Against Epilepsy defines epilepsy as an enduring propensity of recurrent epileptic seizures [5]. These are characterized as symptomatic, hypersynchronous and paroxysmal depolarisations and high-frequency firing of populations of neurons in the CNS [6]. Epileptogenesis are the mechanisms by which a normal brain becomes epileptic. These mechanisms lead to an imbalance between excitation and inhibition, which results in hyperexcitable neuronal population [6]. However, the underlying mechanisms of epileptogenesis are not fully understood. Epileptogenesis includes several hallmarks, such as neuronal death, gliosis, inflammation and re-wiring, among others [7].

Although there are an increasing number of treatment options, there is still no cure for epilepsy. Anti-epileptic drugs (AEDs) are the principal treatment and its basic mechanism is to restore the balance between inhibitory and excitatory transmission, leading to the suppression of seizure generation [8]. Thus, it is relevant to highlight that most of the actual treatments are directed to neurons. However, the current antiepileptic drugs have two major drawbacks. First, recent studies have shown that only 70% of the patients can be successfully treated. Therefore, 30% of the cases have refractory epilepsy [9]. Secondly, the AEDs have risks of cognitive complications [10]. Furthermore, the current available AEDs are mainly symptomatic, since they

only block seizures. AEDs do not affect the underlying pathology or progression of this disorder and it is therefore imperious to discover new therapies in order to prevent its onset and/or progression [11].

Traditionally, epilepsy has been considered only a neuronal disease. However, a new direction was taken to fully understand the mechanisms of this neurological disorder [12]. In the last decade, researchers have been dedicated to the excitatory and inflammatory effects of glia cells in this pathology. The direct neuromodulatory actions of inflammatory mediators, such as cytokines have been particularly explored [13].

1.3 Temporal Lobe Epilepsy

The hippocampus, compared to other structures, is an exquisitely seizure-prone structure [14], since the principal cells, within this structure, display propensities for epileptiform activity and seizures. However, it is not yet clear, whether the epilepsy is caused by hippocampal abnormalities or whether the damaged in hippocampus is due to cumulative effects of seizures [15]. In terms of anatomy, the hippocampus belongs to the limbic system and is located under the temporal lobes of the cerebral cortex.

Temporal Lobe Epilepsy (TLE) is one of the most dangerous and frequent types of intractable epilepsy [16,17] and it has the most common structural abnormality in human epilepsy, defined as hippocampal sclerosis (HS) [17,18]. HS consists of hippocampal atrophy involving an extensive and selective neuronal loss and gliosis, mostly in cornus ammonis (CA) 1 and dentate gyrus (DG) regions [19]. Reactive gliosis is characterized by hypertrophy of glial cells [10]. Another alteration in HS includes an aberrant mossy fiber sprouting, in which the mossy fiber axons of DG cells form synapses with themselves and with other granule cells (synaptic reorganization) [20–22], thus creating a monosynaptic excitatory feedback [16,23,24]. Actually, this feature has been noted in both animal models of epilepsy [25] and in human brain tissue from TLE patients [26].

Although TLE is an epileptic disorder that does not feature a typical inflammatory pathophysiology, there are several evidences supporting the occurrence of an inflammatory state sustained by microglia, astrocytes and neurons and also by the presence of pro-inflammatory mediators [27].

1.4 Neuroinflammation

Inflammation is defined as a homeostatic phenomenon, consisting in the quick production of pro-inflammatory or anti-inflammatory mediators by both innate and adaptive immunity cell types [28].

The CNS has historically been considered an immune-privileged site [29], since immune responses were thought to be constrained by the blood-brain-barrier (BBB) [27,30]. This anatomical structure assures the separation between the nervous tissue and the peripheral environment [31], protecting the brain and maintaining its homeostasis [32]. Nowadays, the existence of immune and inflammatory reactions in the CNS and their role in the development and progression of multiple neurodegenerative disorders has become clear [33]. Moreover, the CNS is constituted by its own innate immune cells, the microglia cells, which constitute a major player of innate immune mechanisms [34,35].

In most cases, neuroinflammation constitutes a beneficial process, being defined as a defense mechanism aimed to protect the CNS against insults such as infection, injury or trauma [36]. This process is a result of resident parenchymal cells activation, such as microglia, astrocytes, and neurons, as well as via infiltration of immune cells from the periphery [37]. The beneficial effects include the clearance of cellular debris and secretion of neurotrophic factors and cytokines [37]. Whenever inflammatory process and immunosuppressive (e.g, tissue regeneration) pathways gets out of balance, a chronic neuroinflammation may arise. In this situation, inflammation becomes detrimental for brain tissue and results in cell dysfunction or death, contributing to the pathogenesis of several neurological conditions[36,38,39].

Over the last decade, as a result of supportive evidence in experimental models and in the clinical studies, the role of inflammation in the pathophysiology of seizures and epilepsy has received an increasing attention[40]. One major hallmark of neuroinflammation is the activation of glial cells, named reactive gliosis [41], which is also a characteristic frequently encountered in TLE patients and in epilepsy animal models [13,42,43]. Both clinical and experimental evidences suggest a direct and reciprocal relationship between glia-mediated inflammatory processes and neuronal excitability and epileptogenesis [27,44-45]. Thus, inflammation can be the consequence of recurrent seizures, as well as the cause of the underlying pathology [39]. Experimental studies demonstrated that several insults can induce a cascade of chronic inflammatory processes in the CNS, which contribute to the development of epilepsy [46,47]. This event is often associated with

neuronal cell death. In turn, the recurrence of spontaneous seizures can maintain the inflammation [48]. Inflammation can be induced by seizures and can persist for days, even after the termination of seizures [49-51]. However, the mechanisms that lead to seizure-evoked inflammation are still unknown [52]. Although cell loss does not induce inflammation in this context, dying cells may contribute to the perpetuation of the inflammatory process[47,53]. Noteworthy, most of neurodegenerative diseases are also characterized by the production of inflammatory mediators, such as cytokines [54-56].

1.5 Glial cells

Glia cells are involved in diverse neuronal functions, being the main role the support to the neurons during brain development and function [57]. In CNS, glial cells can be divided into four major categories: microglia, astrocytes, radial glial cells, and oligodendrocytes [58]. This study will focus in microglia and astrocytes, since these are the glial cells activated in pathological conditions.

Nowadays, astrocytes have been considered to be functionally associated with the pre- and postsynaptic nerve terminals, as the third element of a structure known as "tripartite synapse" [59,60]. In the healthy brain, astroglia play a pivotal role in synapse regulation through metabolic processes, established in cooperation with neurons, such as energy supply and also synthesis and removal of neurotransmitters[61-65]. The production of inflammatory mediators (e.g., cytokines) by astrocytes is also involved in the regulation of synaptic activity [64]. Several other functions have been attributed to astrocytes, such as ion homeostasis and tissue repair [66,67].

Microglia are the innate immune cell of the CNS, located within the brain parenchyma, in structures like hippocampus [64,68]. These glial cells provide a defense in CNS against several pathological insults and have multiple morphological and functional profiles influenced by their surrounding environment [69-71]. Normally, microglia cells are in a surveying (resting) state, monitoring their environment with a ramified morphology, resembling the dendritic cells from the innate immune system [72]. In this state, microglia are able to sense neuronal and astrocytic activity and other physiological changes such as pH shifts, ion currents and neurotransmitter release[37-73]. Whenever activated, in response to injuries or to immunological stimuli, microglia change rapidly to a prime state (characterized by shortened processes and a rounder cell body) and subsequently to an amoeboid activated state [74]. This morphology enables microglia to migrate, through the parenchyma toward the lesion sites, and to release inflammatory

mediators, such as cytokines [75]. Only in the active state, microglia display endocytic and phagocytic activity and serve as antigen-presenting cells [30,37]. Phagocytic activity plays a beneficial effect, as the regulation of homeostasis, through the clearance of cellular debris and/or toxic substances [76]. Moreover, due to their proliferation ability, microglial cells can also increase in number in response to a stimuli [77]. These immune cells have a dual activity, since they can either promote neuronal survival and regeneration or contribute to neurodegeneration.

Astrocytes, together with microglia, are responsible for the inflammatory and immune responses in the brain. Being astrocytes the major glial cell type of the CNS, researchers point to a great role played by these cells in neuroinflammatory processes [29]. It has been demonstrated that astrocytic cells initiate and amplify inflammatory-mediated mechanisms involved in several human CNS diseases, including epilepsy [78,79]. Studies, both *in vitro* and *in vivo*, argument that astrocytes are a major source and target of epileptogenic inflammatory signaling [80]. Likewise, in response to an insult or stress, astrocytes become reactive (activated), leading to the release of inflammatory mediators and growth factors that help regulate and resolve the inflammatory tissue response [63,75]. However, in these situations, astrocytes do not respond as fast as microglia [81]. Astrocytes proliferate and extend their processes around the injury site, which ultimately results in a scar formation [67,82,83].

Since glia cells are implicated in the modulation of synaptic transmission, it is plausible to point that alterations in these cells may have a functional role in the hyperexcitability [84]. In fact, alterations in the neurotransmitters cycle and induction of inflammatory molecules in epilepsy have been associated with glial cells' activation (cytokines' effects in epilepsy in section 1.6) [27,85,86] . Consistent with this, manipulations of glial inflammatory processes are being considered as potential therapeutic targets for epilepsy.

1.6 Cytokines

Cytokines are considered as one of the primary classes of inflammatory regulators of innate and adaptive immune responses throughout the body, including the CNS [87]. Being signaling molecules, cytokines act through specific receptors and signal transduction pathways to exert a particular biological response in the target cell [69]. Although all cell types in the brain are capable to express cytokines and their respective receptors, its basal level of expression is quite low [27]. However, followed CNS insults, cytokines are quickly overexpressed [27]. Cytokines' actions can be neuroprotective or neurotoxic in neurological diseases. For example, the transcriptional

pathway induced by cytokines can modulate cell death and survival and also synaptic reorganization and plasticity [88].

In epilepsy, the overproduction of cytokines appears to be implicated in synaptic dysfunction, as well as in excitotoxicity and apoptotic neuronal death[47,89,90]. Excitotoxicity is a process of neuronal death triggered by excessive or prolonged activation of excitatory neurotransmitter receptors [91]. This suggests that the release of cytokines by glia cells during seizures may contribute to seizure-mediated neuronal damage[52]. Regarding synaptic dysfunction, these inflammatory mediators have effects in the seizure threshold and in epileptic activity, which are important evidences that neuroinflammation has a vital role in the development of epilepsy[52]. The cytokine effects' on neuronal survival and excitability seems to be mediated by interactions between these proteins and neurotransmitters [52].

Several studies point to interleukin-1β (IL-1β), tumor necrosis factor-alpha (TNF-α) and interleukin-6 (IL-6) as the principal pro-inflammatory cytokines involved in seizure generation and propagation [49,92-94]. Concerning other cytokines, there is still limited information about their role in seizure phenomena [34,95].

1.7 IL-1β

The pro-inflammatory cytokine IL-1 is a pivotal regulator of immune responses to pathogens and to injury and, not surprisingly, it has similar effects within the CNS [96]. All the IL-1 family members are present within the brain [97], being IL-1β the most studied IL-1 in neuroinflammation and epilepsy [98,99].

IL-1β is synthesized as a 31 kDa inactive precursor (pro-IL-1β) [100]. Therefore, to become the bioactive 17 kDa form, the pro-IL-1β requires an enzymatic cleavage, by caspase-1, also known as IL-1β converting enzyme (ICE). The biological function of both IL-1β is mediated through the binding to interleukin-1 receptor type I (IL-1RI), which induces an association with the receptor-accessory protein (IL-1RAcP). This complex is able to initiate an intracellular signal through an adaptor protein, myeloid differentiation factor 88 (MyD88) [100,101]. This is followed by an activation of several transcription factors, such as nuclear factor-κB (NF-κB), mitogen-activated protein kinases (MAPKs), among others [101]. IL-1β is considered a pivotal mediator, not only because of its ability to upregulate other inflammatory cytokines, such as IL-6 and TNF-α, but also because it is the first cytokine released in pathologic conditions [100,102].

A strong activation of IL-1β/IL-1R1 complex was already described in both glial and neuronal cells in the analysis of human brain specimens of TLE patients with hippocampal sclerosis [103,104]. Furthermore, and regarding IL-1β effects in synaptic transmission, an enhancement of neuronal excitability and also a decrease in seizure threshold were described in hippocampus and other seizure sensitive regions [105,106]. Therefore, IL-1β is classified as pro-convulsive molecule, while inhibitors of its pathway may be powerful anticonvulsants [107].

1.8 TNF-α

TNF-α is a pleiotropic cytokine, playing pivotal roles in immunity, cell proliferation, differentiation and cell death through the activation of several downstream signaling cascades [108].

TNF is synthesized as a 26 kDa transmembrane protein precursor (mTNF) and cleaved into a 17-kD mature soluble form (sTNF) by the metalloprotease TNF-α converting enzyme (TACE) [109]. The biological effects of TNF-α are mediated through the interaction with transmembrane receptors, namely TNF receptor type 1 (TNFR1 or p55) and type II (TNFR2 or p75) [108]. Whereas TNFR1 is expressed in the majority of CNS cell types and activated by both mTNF and sTNF, TNFR2 is mainly expressed in microglia cells and only activated by mTNF [110].

There are two main groups within the TNFR superfamily of receptors. The first group induces cell death signaling and is only carried out through TNFR1 (p55), since TNFR2 (p75) lacks a functional death domain (DD). Thereby, TNFR2 only signals for anti-apoptotic reactions, leading to the production of neurotrophic, neuroprotective and anticonvulsant factors [34]. The TNF-α/TNFR1 complex is able to recruit several members of the caspase family of cell death proteases, such as the initiator caspase-8 and -10, which cleave effector caspases, particularly caspase-3 [111,112]. The second group can be constituted by both receptor types whenever they present the TRAF interacting motifs (TIM) domain, which binds to TNFR-associated factors (TRAFF) [113]. The signal is carried out through this complex by the activation of transcription factors, such as NF-κB, Jun N-terminal kinases (JNK), and MAPKs [108]. Recent studies have shown that, like IL-1β, TNF-α possesses neuromodulatory properties and is, thereby, able to increase neuronal excitability through several effects in neurotransmission mediated by TNFR1 [114,115]. The consequence of TNF-α on seizures and on the determination of inflammatory processes towards neurodegeneration or neuroprotection, seems to depend on its level in the

brain and which receptor type is predominantly activated [69]. In fact, TNFR1 is described as a pro-ictogenic factor, while TNFR2 plays an anti-ictogenic role [114].

1.9 IL-6

IL-6 is also recognized as a pleiotropic cytokine that was originally classified as a pro-inflammatory cytokine. However several discoveries indicated that this interleukin has also anti-inflammatory properties [116]. IL-6 has emerged as a key player in the nervous system, which is evident from its involvement not only in neuroinflammation, but also in several nervous system pathologies [116].

This cytokine exerts its biological functions by binding to the non-signaling IL-6 receptor (IL-6R). Therefore, the recruitment of additional receptor proteins is necessary to induce the signaling pathways [117]. The IL-6/IL-6R complex specifically triggers the homodimerization of glycoprotein 130 (gp130) with the alpha subunit of IL-6R. This, in turn, activates IL-6 signal transduction through intracellular tyrosine-kinases such as Janus kinases (JAK-1 and JAK-2) [110,117,118].

Similarly to IL-1β and TNF-α, IL-6 is rapidly produced by glial cells during seizure activity [48]. However, astrocytes are considered the major producers of this cytokine [116]. Various studies have emphasized the role of this cytokine in the initiation of inflammation, through the production of chemokines, cytokines (e.g., IL-1β, TNF-α and IL-6 itself) [119]. In relation to excitotoxicity and seizure generation, IL-6 has a dual effect that appears to depend on its levels in the brain and on the type of cells producing the cytokine, emphasizing the importance of the tissue microenvironment [34,116,117]. However, the mechanisms underlying the protective or destructive effects of this interleukin in neuronal excitotoxicity are not yet completely understood [116]. Noteworthy, the majority of studies describe IL-6 as a neurotrophic factor, with an important role against excitotoxicity-induced neuronal damage [116].

1.10 Cell death

The knowledge of molecular pathways underlying neuronal death are considered very important in epilepsy [111]. Numerous studies performed in both experimental models and in TLE patients showed that repeated or prolonged seizures (status epilepticus) can cause neuronal death within vulnerable brain regions, such as the hippocampus [111,120]. Moreover, evidence

proved that cell death is also able to induce seizures [111]. The main mechanism of epileptic cell damage has been attributed to excitotoxicity, which mainly results from an over-activation of ionotropic glutamate receptors, since glutamate is the principal neurotransmitter in the brain [121]. Excitotoxicity is able to provoke cell death by necrosis and apoptosis [122-124]. Necrosis and apoptosis are two different forms of cell death [125]. Necrosis usually occurs when cells are injured to the point where they are beyond repair and provokes damage to the surrounded tissue [126]. On the other hand, apoptosis is a physiological process of programmed cell death, meaning that, it is cell-autonomous and controlled [124,127], with formation of membrane-enclosed vesicles, known as apoptotic bodies [128]. In contrast to necrosis, apoptosis does not inflict damage to the surrounding tissue and neither induces inflammation [126].

Caspases, a family of cysteine proteases, are the central regulators of apoptosis. Two major caspase-dependent pathways have been described. The intrinsic pathway, considered as the most relevant to seizure-induced neuronal death, is activated by several intracellular stressors, and ultimately leads to initiator caspases (e.g., caspase-9) activation, which processes the downstream effector caspases (e.g., caspase-3, -6, and -7) [120,129-131]. The extrinsic caspase pathway is activated by cell surface-expression of death receptors of TNF superfamily [132]. Upon binding to its receptors, TNF recruits intracellular adaptor proteins such as Fas-associated death domain protein (FADD) or TNFR associated death domain (TRADD) [133]. Then these complexes recruit caspase-8 and -10 followed by the cleaving of effector caspases, particularly caspase-3 [112]. Furthermore, there is also a caspase-independent apoptotic pathway [120]. In this apoptotic-pathway, apoptosis inducing factor (AIF) and calpains seem to be the critical mediators. Calpain is a protease that coordinates the calcium-dependent signaling pathways underlying neuronal death [134].

1.11 Experimental Models of epilepsy

The development and characterization of experimental models has offered an enormous contribution to the knowledge of basic cellular, molecular and electrophysiological mechanisms of epileptogenesis [135,136]. Nevertheless, validated experimental models of epilepsy are essential to gain insights into the neural mechanisms of epilepsy, but also to test the efficacy of new AEDs and novel therapeutic approaches [137]. Given the disadvantages of the *in vivo* models, such as the need for large number of animals, the high mortality, and the relative slow data collection, there is an increasing interest in simpler models of epilepsy [138,139]. *In vitro* models

allow the application of a more detailed and well-controlled variety of methods that would, otherwise, be difficult to employ under *in vivo* conditions [140], while preserving the critical network phenotypic features which generate recurrent seizures [141]. However, these seizure models lack the behavioural and motor components of clinical seizures [140]. Acute brain slices are the most popular *in vitro* preparations. [140]. However, it also has several disadvantages. One of them is the very short viability of acute slices, which only last for a few hours and unable to study chronic epileptogenesis. In contrast, cultures of brain tissue (e.g., organotypic hippocampal slice culture) are considered a long-term preparation, maintaining, over time, many aspects of the *in vivo* context, such as the brain architecture and the functional local synaptic circuitry [142].

1.12 OHSC as a model of epileptogenesis

Over time, the organotypic hippocampal slice cultures (OHSC) have been progressively useful and advantageous for the study of several neurobiological disorders, including epilepsy and neuroinflammation [143,144]. These cultures reproduce and preserve the intrinsic properties and the complex *in vivo* organization of the cellular network [145]. Moreover, they can be maintained for several weeks in an artificial growth medium allowing to follow long time effects [140].

There are two studied methods used to prepare slices cultures: the roller tube, pioneered by Gähwiler [146] and the membrane interface technique, established by Stoppini and co-workers [147]. Usually, the cultures of organotypic slices of hippocampus and cortex regions, are prepared from 6- to 7-day-old pups (P6-7) [148], since at this age the hippocampal cytoarchiture is already established and can then be studied from 7 to 30 days in culture [135]. OHSC are prepared from postnatal rats and do not represent adult tissue [135]. Only after three weeks *in vitro* (21 days *in vitro*) [149], the maturation of the different cell types, synaptic contacts and receptor expression resembles what is observed in the adult tissue [142,150–152]

The trauma of culturing has a profound effect on the survivability of neurons. A robust degeneration of neurons start as early as four hours after culturing and continues up to at least 6 DIV followed by a low-level of neuronal death that persists up to at least 28 DIV [153]. Furthermore, the deafferentation that occurs during tissue slicing, leads also to some reorganizational processes, which are also observed in chronic epileptic rats [154] and epilepsy humans patients [155]. These reorganizational processes include: mossy fiber sprouting and formation of recurrent excitatory connectivity (also a feature of TLE) and reorganization in

CA1 region [156-160]. As a consequence of these alterations, excitatory activity progressively increases during culture time and epileptogenesis may be initiated [159,161,162]. Therefore, OHSCs may provide a model of chronically epileptic tissue, since the development of abnormal connectivity in the organotypic slices mimics the aberrant connectivity found in the epileptic brain [135]. Despite these morphological features, spontaneous epileptiform activity without pharmacological induction has rarely been reported in OHSC [163]. However, recently, some groups described in detail the functional characterization of spontaneous development and evolution of epileptiform activity within OHSC, which were maintained in an artificial growth medium without serum (Neurobasal A supplemented with B-27) [164,165]. A high incidence of spontaneous epileptiform activity was recorded in OHSCs from 7 to 30 DIV. Other features related to TLE, such as the latent period and anticonvulsant resistance, were also reported [141,164].

Taken together, the electrophysiological and morphological abnormalities described so far make the OHSC a simple and powerful system that can allow the study of cellular and molecular mechanisms involved in the mechanisms of epileptogenesis. Hopefully, it will bring us one step closer toward the development of novel therapeutic approaches.

2 AIMS

Research directed toward the therapeutic benefits of anti-inflammatory agents is now considered crucial on the ongoing search for novel antiepileptic drugs [167]. Targeting inflammatory pathways, is regarded as a novel option for the development of biomarkers [168] and therapies for epilepsy [12]. Thus, a full knowledge about the crosstalk between neuroinflammation and epileptogenesis is imperative.

In this work the organotypic hippocampal slice model of epileptogenesis [164] was used in order to disclosure the impact of spontaneous epileptiform activity upon inflammation. In order to accomplish this, a molecular characterization of inflammatory mediators was carried out. Several topics were evaluated throughout culture time, namely:

- Cell death;
- Astrocytes and microglia activation;
- Transcript expression of inflammatory cytokines, specifically IL-1β, TNF-α and IL-6.

3 MATERIALS AND METHODS

3.1 Animals

Sprague-Dawley rats were obtained from Charles River (Barcelona, Spain). All the procedures were performed according to the European Union guidelines (2010/63/EY) and Portuguese law concerning the protection of animals for scientific purposes. All efforts were made to minimize animal suffering and to use the minimum number of animals.

3.2 Organotypic Hippocampal Slice Culture

In this work, organotypic hippocampal slice cultures were prepared from 6- to 7- days-old Sprague-Dawley rats, according to the interface culture method [147]. Rats were decapitated, brains were removed and placed, under sterile conditions, in cold Gey's balanced salt solution (GBSS) with 25 mM glucose.

Combined Entorhinal cortex-hippocampi slices were dissected out and sliced transversely at a thickness of 350µm using a McIIwain tissue chopper. Five slices were placed onto porous (0.4 µm) insert membranes (PICM 0305 Millipore, Bedford, MA) and transferred to six-wells culture plates (Corning Costar, Corning, NY) (**Figure 9** in Appendix, section 9.1). Each well was filled with 1mL of medium, containing 50% Opti-MEM, 25% Hank's balanced salt solution, 25% heat inactivated horse serum, 25 mM glucose, 100 units/mL of penicillin and 100 µg/mL of streptomycin. The culture plates were maintained in an incubator at 37°C in 5.0% CO_2 and 95% atmospheric air.

After 3 days *in vitro* the culture medium was replaced with 1mL of a chemically defined serum-free medium, Neurobasal A, supplemented with 1mM L-glutamine, 100 units/mL of penicillin and 100 µg/mL of streptomycin, 2% B-27 (contains several hormones, fatty acids and free radical scavengers [169,170] and decreasing horse-serum concentrations until a serum-free condition was reached at 9 DIV (**Figure 10** in Appendix section 9.2). Since several amino acids are rapidly consumed within 2 days [171] and glutamine spontaneously degrades, generating a toxic product (ammonia) [172], Neurobasal A-based medium was changed every second day, for three weeks (21 DIV). All experimental assays were carried out at 7, 14 and 21 DIV.

3.3 Propidium iodide (PI) uptake assay

Cell death in OHSCs was evaluated by the cellular uptake of the fluorescent dye propidium iodide (PI). Staining in OHSC is simpler because the dye can be added to the culture medium [140]. PI only enters cells with damaged membranes, and when bound to nucleic acids it allows to see the damaged cells brightly fluorescent (absorbance at 530nm and emission at 620nm) [173]. PI is not toxic to cells and has been widely used as an indicator of neuronal membrane integrity and cell damage [145]. The slices at 7, 14 and 21 DIV were incubated with 2µM sterile propidium iodide solution (Sigma, St. Louis, MO, USA) for 4 hours before imaging. Cellular uptake of PI was recorded in a widefield fluorescence microscope (Axiovert 200, Zeiss, Germany) using an EC Plan-NeoFluar 5x objective, a rhodamine filter and a digital camera. 50 ms exposure time was used in all assays. For quantitative assessment of neuronal damage, the regions of interest (CA1, CA2/CA3 and DG) were delineated using the software application ImageJ (NIH). The intensity value of each analyzed region was obtained by correction with a fluorescence background image. This assay does not discriminate between necrosis and apoptosis.

3.4 Western blot

3.4.1 Tissue lysates

In this study, Western blot analysis was performed in order to address expression changes of proteins related to cell death and also in glial cell markers.

Hippocampi were dissected from 4-5 slices and cell lysis were performed in 150 µL of RIPA (Ristocetin Induced Platelet Agglutination) buffer containing 50mM Tris pH 8.0, 1mM EDTA (Ethykenediamine Tetraacetic Acid), 150mM NaCl, 1% NP40 substitute (Nonyl phenoxlpoylethanol, from Fluka Biochemika, Switzerland), 1% SDS (Sodium Dodecyl Sulfate) and 10% glycerol. During extraction, protein degradation is prone to occur due to endogenous proteases released upon cell disruption. Thereby, RIPA buffer was supplemented with protease inhibitors (Complete Mini-EDTA free, Roche, Germany) and 1mM PMSF (phenylmethysulfonyl fluoride). Cell suspension was left shaking during 15 min at 4ºC and the insolubilized fraction was removed by centrifugation, 11000g for 10 min at 4ºC. Finally, the supernatant was collected and stored at -20ºC for further use.

Total protein was quantified with the BioRad DC Protein assay Kit, using BSA (Bovine Serum Albumin) as standard. Before samples were loaded onto the gel, they were submitted to a temperature of 95ºC for 10 min in order to denature the higher order structures, while retaining sulfide bridges.

3.4.2 Western blot assay

Samples (40μg of protein per lane) and protein size markers (Precision Plus Protein Standars, Bio-Rad) were run on a standard 12% SDS-PAGE and electrotransferred onto a PVDF membrane (Millipore) at a constant voltage of 150 V for 1h30.

Membranes were blocked for 1h with 3% BSA in TBS-T (20mM Tris base, 137mM NaCL and 0.1% Tween-20) at room temperature. Subsequently, membranes were probed with the primary antibodies (**Table 1** in Appendix section 9.3), diluted in TBS-T with 3% BSA, overnight at 4°C. Finally, membranes were incubated for 1h at room temperature, with goat anti-rabbit, donkey anti-goat or donkey anti-mouse secondary antibody (1:10000, Santa Cruz Biotechnology) linked to HRP (Horseradish Peroxidase). Development of signal intensity was carried out using ECL Plus Western Blotting Detection System (Amersham-ECL Western Blotting Detection Reagents from GE Healthcare, Buckingamshire, UK) and detected using X-Ray film (Fujifilm). The relative expression of the protein bands was accomplished with Image J software and standardized for GAPDH (Glyceraldehyde 3-phosphate dehydrogenase) levels. Protein levels at 14 and 21 DIV were normalized to 7 DIV levels.

3.5 qPCR

3.5.1 RNA isolation and quantification

RNA was extracted from OHSCs according to QIAGEN RNeasy Mini Kit (Qiagen). Slices, were defrosted in 1ml of QIAzol Lysis reagent with a TissueRuptor homogenizer, previously DEPC-treated. Quantification of total RNA was accurately determined using Nanodrop 1000 (ND-1000 Spectrophotometer, Thermo Scientific).

3.5.2 Reverse Transcription reaction

Two reaction mixes were prepared to perform the in vitro reverse transcription (RT) reaction: 1) RNA mix containing 2 µg of total RNA, 1 µL of random primers and 1 µL dNTPs, in a total volume of 10 µl; 2) SuperScript mix containing 25 mM $MgCl_2$, 0.1M DTT (Dithiothreitol) and SuperScript II reverse transcriptase buffer in a total volume of 10 µl. RT-PCR was carried out in a thermoclycler (MyCycler – Bio-Rad, Hercules, CA 94547).

First RNA was heated for 5 min at 65 ºC and chilled for 2 min at 4ºC, followed by the addition of the SuperScript mix. When temperature reached 25 ºC, 50 units of SuperScript II Reverse transcriptase (EC 2.7.7.49, Invitrogen, Carlsband, CA, USA) was added followed by 60 min at 42 ºC (optimal SuperScript II temperature). Reaction was terminated by inactivating the enzyme for 20 min at 72 ºC.

For each RNA sample a reverse transcription reaction was carried out in the absence of reverse transcriptase in order to ensure that product amplification did not arise from genomic DNA.

3.5.3 Relative quantification

cDNA amplification was performed in a Rotor-Gene 6000 real-time rotary analyzer thermocycler (Corbett Life Science, Hilden, Germany) in the presence of SYBR Green Master Mix (Applied Biosystems, Foster City, CA, USA) and 0.2 µM of each specific gene primer (**Table 3** in Appendix section 9.4). The amplification of cDNA was carried out by the following program: an initial denaturation for 2 min at 95ºC, 50 cycles with 30s at 94ºC, 90s at 60ºC and 60s at 72ºC, followed by a melting curve to assess the specificity of the reactions. The Ct (Cycle Threshold) and the melting curves (**panels C** of **Figures 14-21**) were acquired with Rotor-gene 6000 Software 1.7 (Corbett life Science). In order to determinate the PCR efficiency (E) for each gene, which is needed for relative quantification by comparative Pfaffl method, a qPCR with cDNA samples from 5-fold sequential dilutions of cDNA was performed for each set of primers. In all experiments GAPDH was used as a reference internal gene. For each gene, replica reactions were performed and the mean of two reactions was used to calculate the corresponding expression level. Two types of negative controls were run with samples, 1) no reverse transcription control, which used cDNA obtained in the absence of SuperScript II and 2) no template control, which did not contain cDNA.

3.6 Gel electrophoresis

The electrophoresis was performed in a 2% agarose gel in TAE buffer (Tris-acetate-EDTA: 20mM glacial acetic acid, 40 mM Tris base and 1 mM EDTA) with 0.05 µL of GelRed (Invitrogen, Biotechnology) per 1 mL of TAE. After amplification in Rotor-gene 6000, 15µL of each PCR product plus 3µL of loading buffer (6x NZYDNA loading dye, Nzytech) were loaded on the agarose gel. Molecular weights of cDNA were assessed by running, alongside, a marker for DNA size (5 µl) (NZYDNA Ladder V, Nzytech).

3.7 Immunohistochemistry (IHC)

3.7.1 Immunohistochemistry

Slices were fixed for 1h with 4% paraformaldehyde (PFA) diluted in phosphate-buffer solution (PBS) at room temperature, followed by an incubation in increasing concentrations of a sucrose solution (10% and 20% in PBS) at room temperature and lastly slices were kept in 30% sucrose solution at 4ºC until further use.

Slices were cut out of the insert and put in slides (2 slices per slide). Each slice was surrounded with DAKO pen (Dako, Denmark) to protect staining areas from drying out and from mixing with each other. Followed PBS washes, slices were incubated for 3h at room temperature in blocking solution containing 10% BSA 10% Horse Serum and 1% Triton X-100 in PBS, which ensure simultaneous blocking and permeabilization of the tissue. Subsequently, slices were incubated with the primary antibodies (**Table 2** in Appendix section 9.3) diluted in blocking solution for 48h at 4ºC. Slices were rinsed with PBST (PBS containing 0.1% Tween-20) and the secondary antibodies, coupled to fluorophores (donkey anti-rabbit Alexa Fluor 488, donkey anti-goat Alexa Fluor 488 or donkey anti-mouse Alexa Fluor 568, 1:400, Invitrogen), were applied to the slices for 24h at room temperature. The nuclei were stained with Hoechst 33342 (1:100 dilution in PBS from a 2mg/mL stock; Invitrogen) for 40 min at room temperature and then washed. The coverslips were mounted in Mowiol (40 µL per slice), which is a non-absorbing compound without autofluorescence and light scattering, and is, therefore, considered adequate for fluorescence microscopy. Finally, slices were imaged with a confocal laser scanning microscope (LSM 710, Zeiss, Germany), using an EC plan-NeoFluar 5x to obtain images of the whole hippocampus and a Plan-Apochromat 20x objective (Zeiss, Germany) to achieve specifically images from DG, CA3 and CA1 regions.

4 RESULTS

4.1 Cell death

As already mentioned, cell death and neuroinflammation are closely associated [27,124]. In order to characterize cell death in the OHSC model of epileptogenesis an evaluation by PI uptake and αII-Spectrin cleavage was carried out. Assays were performed at 7, 14 and 21 DIV.

4.1.1 PI uptake

PI uptake in DG, CA3 and CA1 regions of organotypic slices was measured. The three analyzed time points show PI-positive cells in all regions of the hippocampus (**Figure 1A**), which corroborates the occurrence of cell death. The lower PI uptake was observed at 7 DIV slices, while the maximum cell death occurred at 14 DIV slices (**Figure 1B**). When comparing 7 and 14 DIV slices, all regions show a significantly higher level of PI uptake in 14 DIV slices (DG: 33.39 ± 4.13 vs 107.1 ± 9.86; CA3: 22.59 ± 2.89 vs 133.1 ± 9.79; CA1: 59.16 ± 4.07 vs 160.2 ± 11.90, ***$p<0.001$) (**Figure 1B**). Regarding 14 and 21 DIV slices, CA3 (133.1 ± 9.79 vs 54.24 ± 10.04, **$p<0.01$) and CA1 regions (160.2 ± 11.90 vs 98.69 ± 9.63, *$p<0.05$), show a significant decrease of PI uptake in 21 DIV slices (**Figure 1B**). In DG, a significant increase in PI uptake was observed from 7 to 14 DIV slices, as pointed out above, while no differences were obtained between 14 and 21 DIV slices (107.1 ± 9.86 vs 101.0 ± 14.96, $p>0.05$) (**Figure 1B**). Overall, the CA1 was the region that suffered the highest cellular damage at all three evaluated time points (**Figure 1B**).

4.1.2 αII-Spectrin cleavage

Characterization of cell death was also assessed through the evaluation of αII-Spectrin cleavage and Pro-caspase-3 activation by a western blot assay, carried out with protein extracts obtained from the hippocampal region of the slices.

αII-Spectrin is a structural protein of the cell membrane cytoskeleton, being important for membrane stability and cell shape regulation [174]. This cytoskeleton protein is abundant in neurons of the CNS and plays vital roles in neuronal support and synaptic plasticity [175]. In its simplest form, spectrin has a molecular weight of a 250 kDa and it is a major substrate of calcium-dependent proteases, such as calpain and caspase-3. Calpain is involved in necrotic

and apoptotic cell death, while caspase is only activated in apoptosis [176]. Thereby, events as neuronal death and stress or injury, which enhance proteolysis, lead to an increase of spectrin break down products (SBDP) [175]. There is a unique calpain mediated fragment with a molecular weight of 145 kDa (SBDP 145). Caspase-3 mediated alpha II-Spectrin cleavage leads to the formation of SBDP 150, which has 150 kDa. In addition, this product can be further degraded by caspase-3, producing the apoptotic-specific 120 kDa fragment [176]. For this reason, recent works use the SBDP as a potential biochemical marker of cell death in neurodegenerative disorders [177,178]. Since αII-spectrin presence in glial cells is minimal, the SBDP are highly specific for neuronal damaged [174]. The three referenced spectrin breakdown products can be detected by antibodies against αII-spectrin [175], allowing to discriminate which type of cell death process is occurring in OHSC, throughout time in culture.

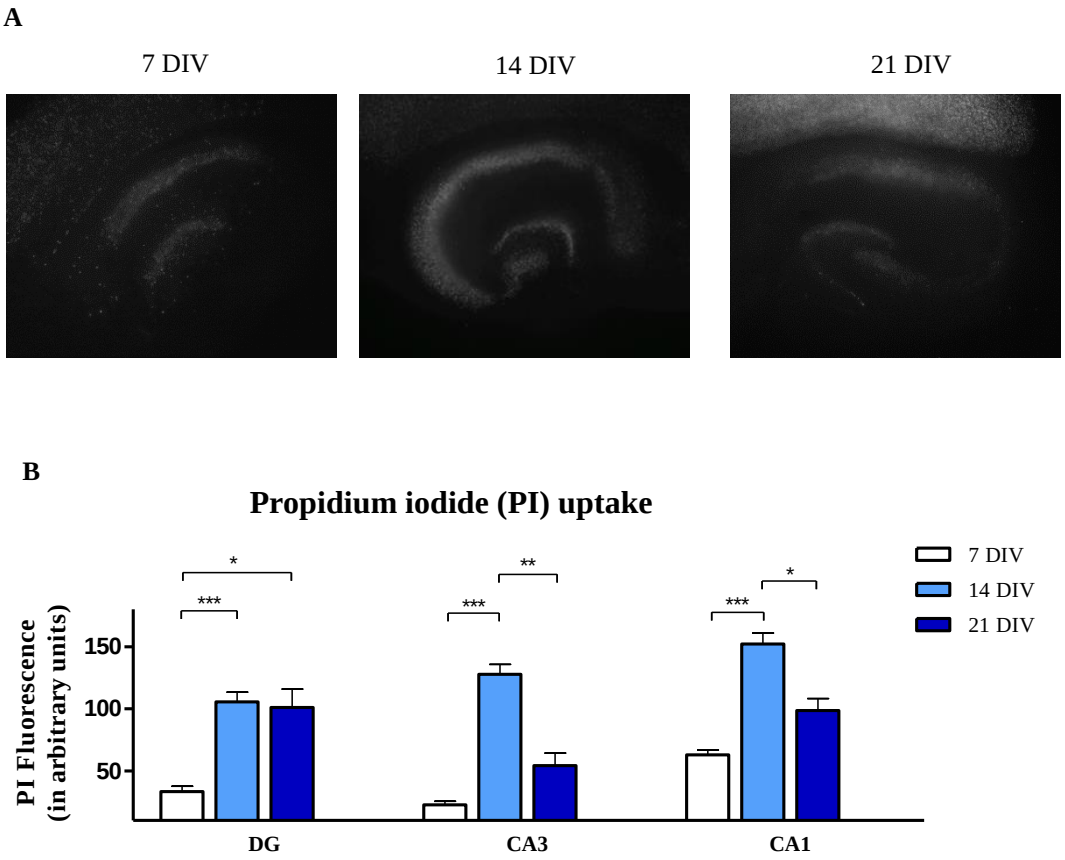

Figure 1| Propidium iodide (PI) uptake in OHSC. A) Representative photomicrograph depicting PI staining show differences in cell death between DG, CA3 and CA1 regions of hippocampus throughout time in culture. **B)** Quantification of PI uptake in each hippocampal region expressed in arbitrary units of fluorescence intensity. All values are mean ± SEM. 9 < slices <30; *p<0.05, **p<0.01, p***<0.001, one way ANOVA followed by Bonferroni's Comparison Test.

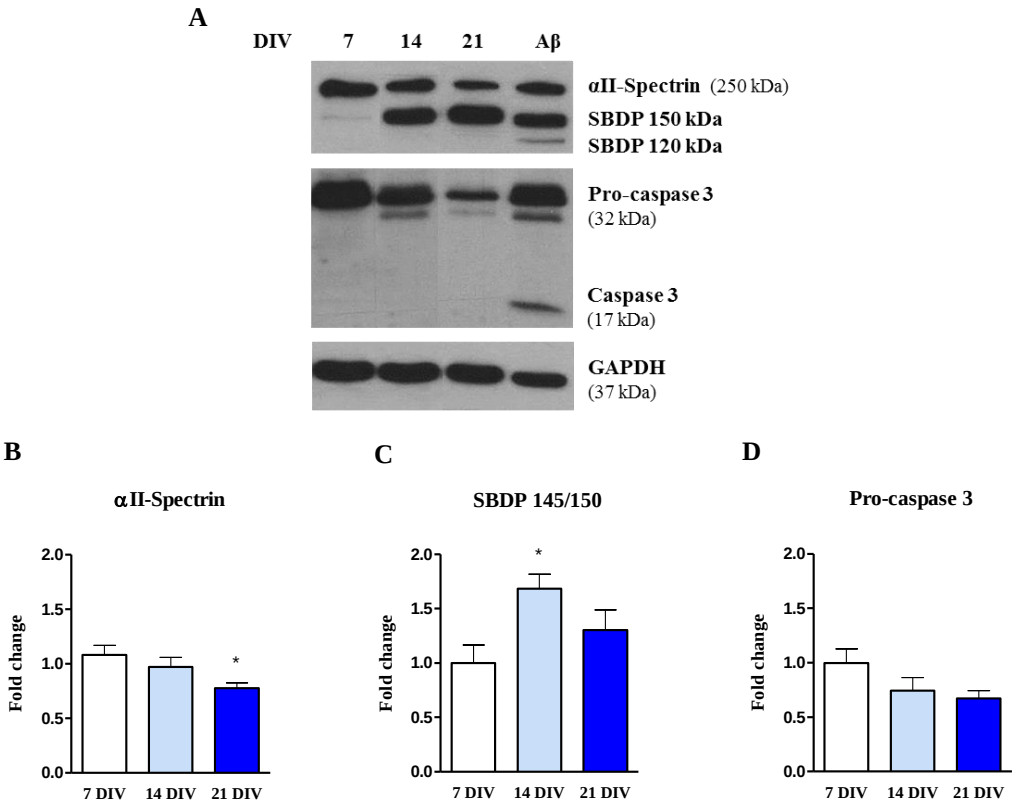

Figure 2| Western blot analysis of alpha-II Spectrin and Caspase-3. A) Representative immunoblots of αII Spectrin and Caspase-3 at 7, 14 and 21 DIV. Lane Aβ, which contains a sample of primary neuronal cultures incubated with Aβ, was used as a positive control of αII Spectrin cleavage and of caspase-3 activated form. GAPDH was used as the loading control. Densitometry analysis of αII-Spectrin **(B)**, SBDP 145/150 (**C**) and pro-caspase 3 (**D**) performed with ImageJ software. All values are mean ± SEM. N=4-8; *p<0.05, one way ANOVA followed by Bonferroni's Comparison Test.

In the three time points studied, full-length αII-spectrin (250 kDa) was detected by western blot analysis (**Figure 2A**). In relation to 7 DIV, a tendency for decreased expression was observed, but with no statistical significance (7 DIV: 1.083 ± 0.0866; 14 DIV: 0.9717 ± 0.08923 and 21 DIV: 0.7771 ± 0.05018; p>0.05) (**Figure 2B**). The expression of SBDP 150 and SBDP 145 was not possible to visualize separately (**Figure 2A**), and since the 120 kDa SBDP, which resulted from the caspase-3 cleavage of αII-spectrin, was absent from all times points, the band visualized at approximately 150 kDa corresponds solely to the calpain-mediated fragment of spectrin (SBDP 145). The expression of SBDP 145 increased significantly from 7 to 14 DIV slices (7 DIV: 1.000 ± 0.1648 vs 14 DIV: 1.685 ± 0.1304, *p<0.05), but no further differences in cell death were obtained from 14 DIV on (14 DIV: 1.685 ± 0.1304 vs 21 DIV: 1.303 ± 0.1841, p>0.05) (**Figure 2C**).

Regarding the caspase-3 immunoblot, a tendency for decreased pro-caspase-3 expression (32 kDa) was detected at 14 DIV (0.7425 ± 0.1209) and at 21 DIV slices (0.6700 ± 0.0723), when

compared to 7 DIV slices (0.9983 ± 0.1298, n=6) (**Figures 2A and 2D**). However, the band corresponding to the active caspase-3 form (17 kDa) was absent in all time points. In order to prove the proper antibody staining, a positive control (lane Aβ), which contain a lysate from a primary neuronal culture treated with Aβ [179], was loaded into the gel. As depicted in **Figure 2A**, this sample shows the presence of SBDP 120 and of the 17 kDa band of active caspase-3. Altogether, these results indicate that the pro-caspase-3 was progressively cleaved but not by an initiator caspase and thus, does not originates the active caspase-3. These results also corroborate the detection of αII-spectrin break down products originated by calpain cleavage only and not by caspase-3 cleavage, and point to the occurrence of cell death by necrosis or through the caspase-independent apoptotic pathway.

4.2 Astrogliosis and microglia activation

Reactive gliosis is considered as a major hallmark encountered both in neuroinflammation and in temporal lobe epilepsy [13,41–43]. Therefore, the astrocytic and microglial activation was evaluated in the OHSC model of epileptogenesis. Glial fribrillary acidic protein (GFAP) is an intermediate filament protein (with cyto-architectural function), expressed specifically in astrocytes. For this reason, GFAP expression has become an astrocytic marker [82]. Moreover, an increased expression of this protein represents the activation of astrocytes [180]. Ionized calcium-binding molecule 1 (Iba-1) is a protein with a localization restricted to microglia [181,182], thus being used as a microglia-specific marker. Calcium-binding protein expression level increases upon microglia activation [182] and it has proven to be helpful in visualizing microglia morphology [183]. Astrocytes and microglia were evaluated through GFAP and Iba-1 expression, respectively, by western blot analysis and by immunohistochemistry assays. The western blot assay was used to evaluate the expression level, while immunofluorescence assay allowed to assess astrocytes and microglia morphology within time in culture.

4.2.1 Analysis by western blot

Although a tendency for increased GFAP protein expression from 7 to 21 DIV was observed (**Figures 3A** and **3B**), no significant differences ($p>0.05$) were achieved between 7 (1.076 ± 0.1135), 14 (1.157 ± 0.0785) and 21 DIV slices (1.263 ± 0.07632). Regarding Iba-1 protein expression (**Figure 3A**), a significant decrease was found in both 14 DIV (0.6240 ± 0.0565, $*p<0.05$) and 21 DIV slices (0.6075 ± 0.0584, $*p<0.05$) when comparing with 7 DIV slices (1.000 ± 0.1388) (**Figure 3C**).

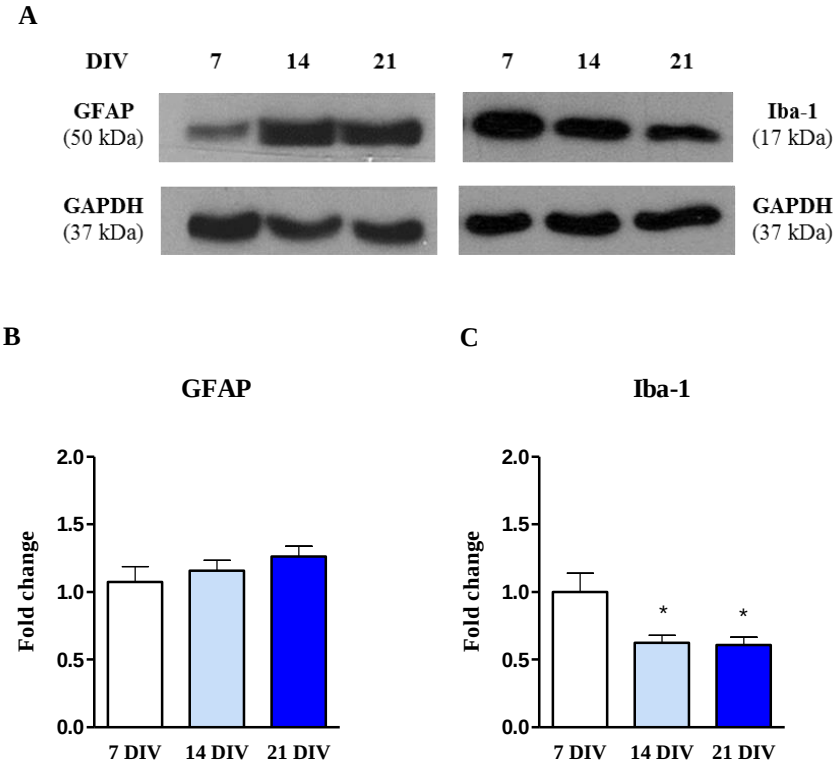

Figure 3| Western blot analysis of GFAP and Iba-1. A) Representative immunoblots of GFAP and Iba-1. GAPDH was used as the loading control. Densitometry analysis of GFAP (**B**) and Iba-1 (**C**) performed with ImageJ software. All values are mean ± SEM. N=6-10, *p<0.05, one way ANOVA followed by Bonferroni's Comparison Test. Statistical tests were performed in comparison with 7 days DIV slices.

4.3 Analysis by immunofluorescence

The following panels depict the immunofluorescence images obtained by the double detection of Hoechst, together with GFAP (**Figure 4**) and Iba-1 (**Figure 5**). An evaluation of glia morphology changes throughout time was performed in DG, CA3 and CA1 regions of the hippocampus. The specific areas where the images were taken are delineated by the dotted line drawn in the image of the whole hippocampus.

4.3.1 Astrocyte activation

GFAP staining at 7 DIV showed a vast number of astrocytes with long and overlapping processes covering the DG and CA3 regions (**Figures 4A2** and **4A3**), resembling a reactive astrocytic scar, as already described [67,82,184]. In CA1 region (**Figure A4**), the morphology characteristic of moderate reactive astrocytes, the hypertrophic cell body with numerous

interdigitated processes, only within individual domain of each astrocyte, can be observed. The astrocytic scar is not yet defined in this region. As the culture time extended, astrocytic processes became longer and ticker in this region. From 14 DIV on, all regions of the hippocampus are covered with astrocytic overlapping processes, which form a dense glial scar (**Figures 4B2-4 and 4C2-4**).

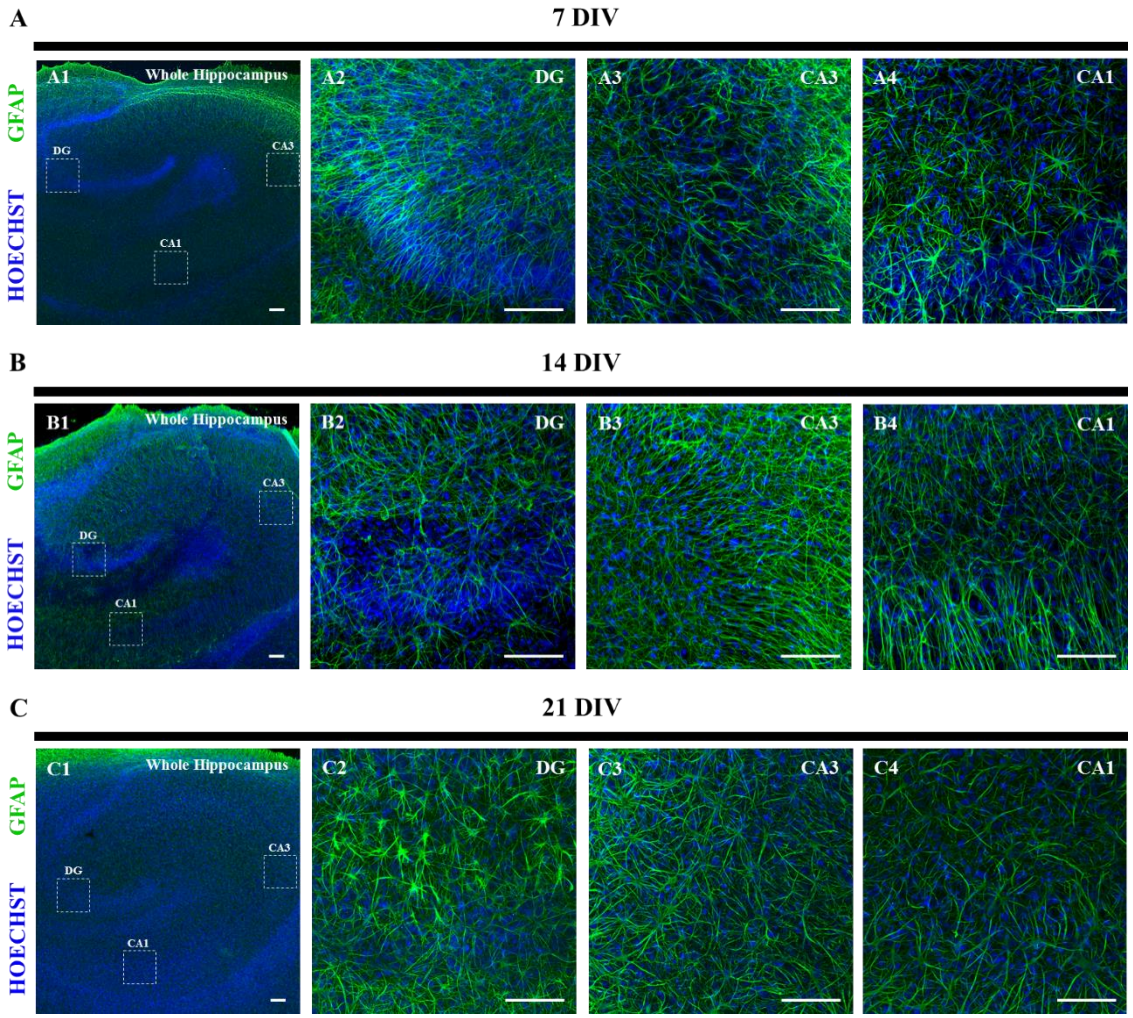

Figure 4| Astrocytes activation in organotypic slices at 7, 14 and 21 days *in vitro* (DIV). Detection of Hoechst stained nucleus (blue), together with GFAP stained astrocytes (green). Confocal images were obtained with a 5x objective (**A1**, **B1** and **C1**) and a 20x objective (**A2-4**, **B2-4** and **C2-4**). The dotted lines delineate the magnified regions. Scale bar, 200µm.

4.3.2 Microglia activation

Regarding microglia, western blot results point to a significant decrease of Iba-1 immunoreactivity throughout time. This decrease is corroborated by the immunofluorescence assay in the images of the whole hippocampus (**Figures 5A1**, **5B1** and **5C1**) and it can be associated with differences in the activation state of microglia cells. At 7 DIV, microglia cells

demonstrate small cell bodies with extensive and thin ramifications in the DG region (**Figure 5A2**), while in CA3 and CA1 regions, microglia displays an amoeboid like morphology with shorter and thicker branches, consistent with an active state (**Figures 5A3** and **5A4**). Concerning microglia morphology at 14 DIV slices, microglia displays a "reactive" form with rounder and larger cell bodies in DG layer, denoting their amoeboid phenotype (**Figure 5B2**). This activated state was not observed in the pyramidal cell region. In fact, when comparing with 7 DIV slices, the microglia in the CA3 and CA1 areas show a reversion to a primed morphology, having an increase of their distal ramifications (**Figures 5B3** and **5B4**). At the last studied time point, the majority of microglia cell population displays a resting ramified morphology with small cell bodies and numerous thin processes (**Figures 5C2-4**).

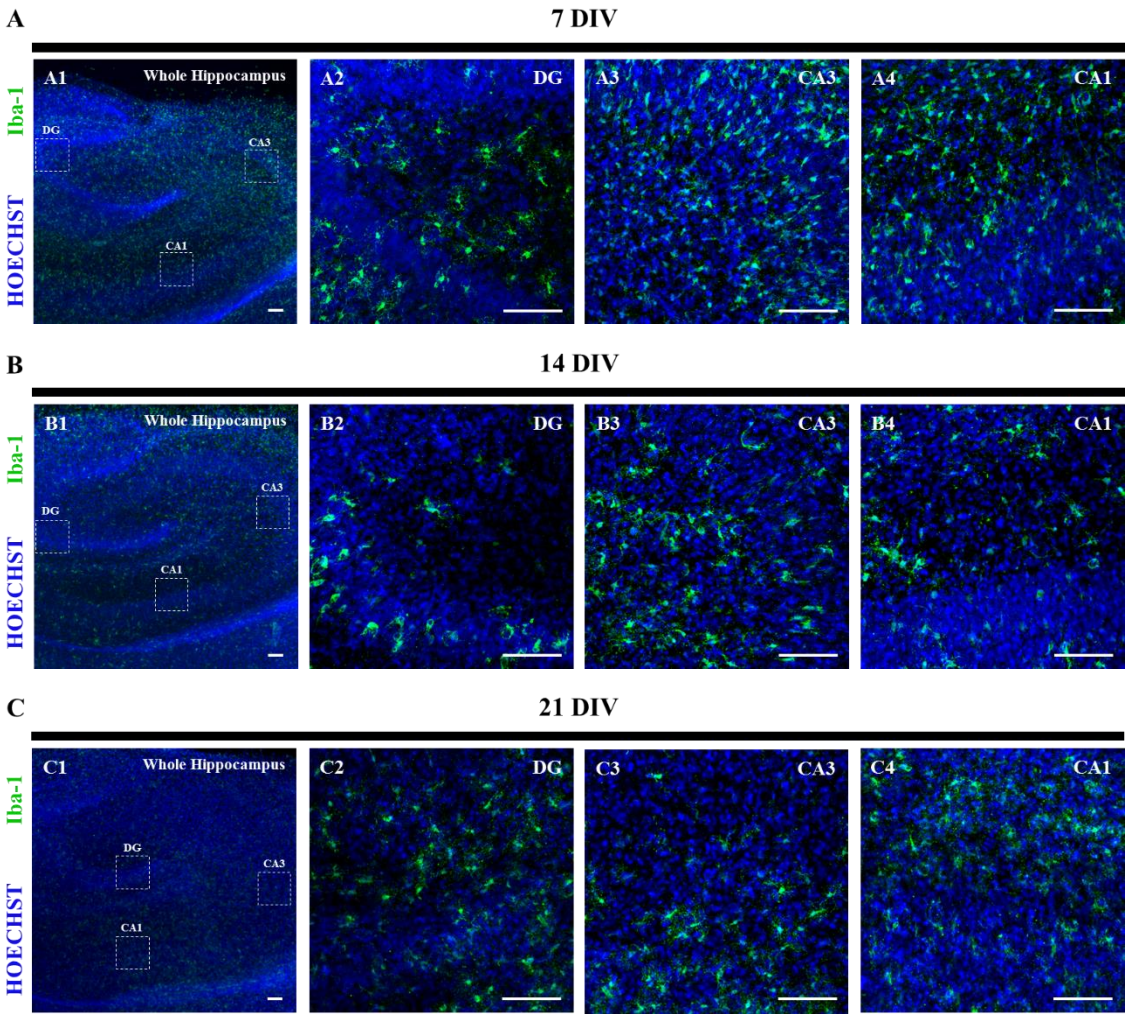

Figure 5| Microglia activation in organotypic slices at 7, 14 and 21 days *in vitro* (DIV). Detection of Hoechst stained nucleus (blue), together with Iba-1 stained microglia (green). Confocal images were obtained with 5x objective (**A1**, **B1** and **C1**) and a 20x objective (**A2-4**, **B2-4** and **C2-4**). The dotted lines delineate the magnified regions. Scale bar, 200µm.

4.4 Inflammatory mediators

Interleukins IL-1β and IL-6, as well as tumor necrosis factor-α (TNF-α), are pointed out as the principal pro-inflammatory cytokines involved in epilepsy. Their expression was found to occur mainly in glial cells [92].

4.4.1 qPCR

This chapter addresses the transcript expression of these cytokines and their respective receptors by qPCR. This assay was performed in samples obtained from organotypic hippocampal slices with 7, 14 and 21 DIV and used specific oligonucleotide primers as detailed in **Table 3** (in Appendix, section 9.4).

4.4.1.1 IL-1β

The transcript analysis of interleukin-1β and IL-1RI showed an increase throughout time in culture (**Figure 6**). In 14 DIV slices, IL-1β increased by 2.240 ± 0.4769 fold, without statistical significance ($p>0.05$) when compared to 7 DIV slices (0.8633 ± 0.2267) (**Figure 6A**). A much higher expression of IL-1β transcript was obtained at 21 DIV with a significant increase of 3.943 ± 0.7372 fold (*$p<0.05$) compared to 7 DIV (**Figure 6A**). Regarding IL-1RI mRNA expression, **Figure 6B** shows a minor increase from 7 DIV to 14 DIV (0.9433 ± 0.1875 vs 1.125 ±0.1051, $p>0.05$). The increase in mRNA expression became significant at 21 DIV, when compared to the first time point studied (1.813 ± 0.2022, *$p<0.05$).

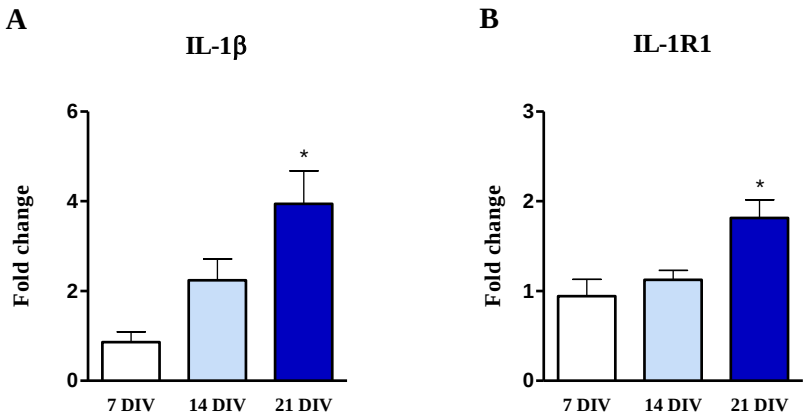

Figure 6| Transcript expression profile of interleukin-1β (IL-1β) and its receptor ILR1. Evaluation of IL-1β **(A)** and ILR1 **(B)** mRNA in slices at 7, 14 and 21 DIV, by relative qPCR. All values are mean ± SEM. *$p<0.05$, N=3-4, one way ANOVA followed by Bonferroni's Comparison Test. Statistical tests were performed in comparison with 7 DIV slices.

4.4.1.2 TNF

TNF-α mRNA levels has also shown an enhancement throughout time in culture (**Figure 7A**). When comparing with 7 DIV slices (1.050 ± 0.1867), TNF-α mRNA levels increased by 1.983 ± 0.0533 fold in 14 DIV slices, but without statistical significance ($p>0.05$) (**Figure 7A**). A much higher expression enhancement was obtained in 21 DIV slices (4.886 ± 0.7347, $^{**}p<0.01$) (**Figure 7A**). The increase in mRNA expression was also significant between 14 DIV and 21 DIV ($^{*}p<0.05$) (**Figure 7A**). Regarding both receptors of this cytokine, an mRNA enhancement throughout culture time was only found in TNFR2 (**Figure 7C**). However, significant difference was only obtain when comparing 7 DIV with 21 DIV slices (7 DIV: 0.8267 ± 0.1445 vs 21DIV: 2.450 ± 0.5103, $^{**}p<0.01$) (**Figure 7C**). The 14 DIV slices solely achieved an increase of 1.307 ± 0.1218 fold for TNFR2 with statistical significance when compared to 21 DIV slices ($^{*}p<0.05$) (**Figure 7C**). The TNFR1 did not show any differences in transcription levels throughout time (7 DIV: 1.008 ± 0.0700; 14 DIV: 1.060 ± 0.0994 and 21 DIV: 1.350 ± 0.2411) (**Figure 7B**).

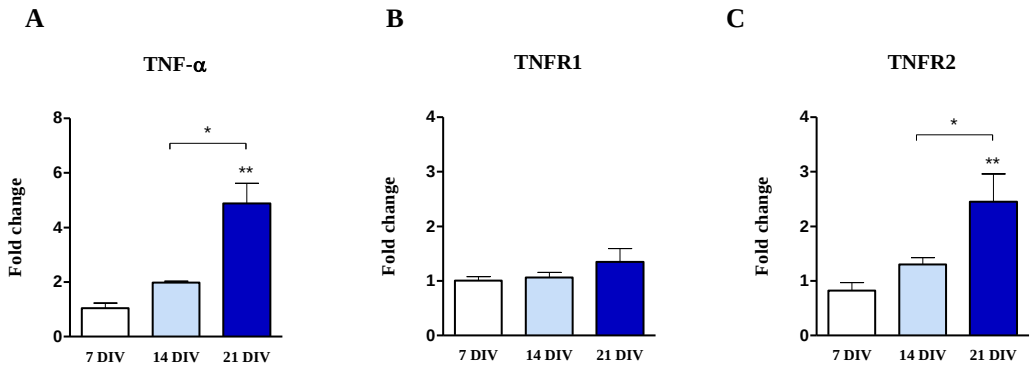

Figure 7| Transcript expression profiles of Tumor necrosis factor alpha (TNF-α) and its receptors (TNFR1 and TNFR2). Evaluation of TNF-α **(A),** TNFR1 **(B)** and TNFR2 **(C)** mRNA in slices at 7, 14 and 21 DIV by relative qPCR. All values are mean ± SEM. $^{*}p<0.05$, $^{**}p<0.01$, N=3-6, one way ANOVA followed by Bonferroni's Comparison Test. Statistical tests were performed in comparison with 7 DIV slices, except if otherwise indicated by the line above the bars.

4.4.1.3 IL-6

Transcript expression of IL-6 did not show a significant difference when comparing 7 with 14 DIV slices (1.043 ± 0.1586 vs 1.127 ± 0.2085, p>0.05) (**Figure 8A**). In contrast, a significant enhancement of 3.514 ± 0.0556 fold in 21 DIV slices was achieved, with a statistical significance of **p<0.01 and *p<0.05 when compared to 7 DIV and 14 DIV slices, respectively (**Figure 8A**). Lastly, IL-6 receptor mRNA levels reached a significant increase (*p<0.05) at 21 DIV (3.213 ± 0.6573), when compared with 7 DIV (0.7467 ± 0.2019) and with 14 DIV slices (1.168 ± 0.2659) (**Figure 8B**). IL-6R mRNA level did not increase from 7 to 14 DIV.

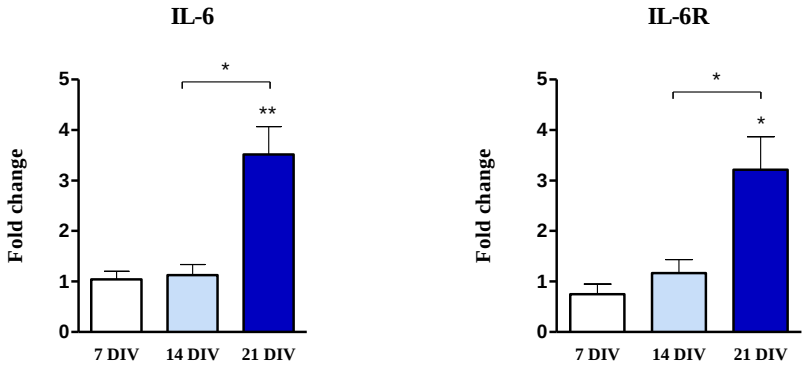

Figure 8| Transcript expression profiles of interleukin-6 (IL-6) and the receptor IL-6R. Evaluation of IL-6 **(A)** and IL-6R **(B)** mRNA in slices at 7, 14 and 21 DIV by relative qPCR All values are mean ± SEM. *<p0.05, **p<0,01, N=3-5, one way ANOVA followed by Bonferroni's Comparison Test. Statistical tests were performed in comparison with 7 DIV slices, except if otherwise indicated by the line above the bars.

5 DISCUSSION

5.1 OHSC as a Model of Epileptogenesis

The study of epileptogenesis is important to gain knowledge about the mechanisms involved in the progression of epilepsy and, ultimately, to acquire new and more efficient therapeutic approaches. Organotypic hippocampal slice cultures share common features with TLE. Also, several features of other experimental models of epileptogenesis are recapitulated in this model, such as the development of abnormal connectivity, the latent period, ictal and interictal activity that underlie the onset of spontaneous seizures, clustering of seizure activity and the development of anticonvulsant resistance [135,185–187]. Noteworthy, all these features are in a compressed time scale, which make the organotypic cultures a less time consuming - low cost model system of epileptogenesis [164]. Therefore, the aim of this project was to use the OHSC to

address the inflammatory progression throughout the course of epileptogenesis, specifically cell death, activation of astrocytes and microglia and expression of inflammatory mediators [140,188,189].

5.2 Cell death

Seizures can be damaging to the brain, particularly if seizures are prolonged (status epilepticus) or repeatedly evoked, leading to neuronal loss in vulnerable brain regions, such as the hippocampus. However, it is important to highlight that the severity of hippocampal cell death is not proportional to the number of seizures or the duration of epilepsy [190]. Excitotoxicity is the main mechanism of seizure-induced neuronal death and it is triggered by the intensive stimulation of excitatory receptors that leads to an uncontrolled overflow of calcium into the neurons, inducing an excitatory response and activation of cytosolic proteases (e.g., calpains and caspases) that participate in cell death signaling pathways [91,175,191-193].

Cell death in hippocampus of TLE patients and in animal models of epilepsy is characteristically asymmetric, being CA1 and DG the most affected regions [24,192]. In fact, the PI uptake assay, in OHSC, was solely confined to the pyramidal and granule cell layers of the hippocampus, which suggests that the majority of dying cells were neurons [111,165]. The majority of cell death was observed in CA1 and it can be associated with the hyperexcitability of neurons and with the effect of sprouting of recurrent CA1 axon collaterals [193]. Moreover, CA1 region has the highest NMDA receptor concentration, therefore excitotoxicity may also be the cause of most cell loss in this hippocampal subfield [194,195]. Furthermore, glial cells release several cytokines that influence cell death (see explanation below) [111]. Regarding cell death progression in OHSC, a peak of cell damage at 14 DIV in both pyramidal and granule layers was observed. This peak of cell death, indicated by PI uptake assay, is in agreement with the highest expression of SBDP 145, a excitotoxic marker, obtained by western blot [174]. Previous work by the group has shown the occurrence of interictal activity at 14 DIV slices, which corresponds to the cell death peak. These results correlate with Staley's group reports in which cell death, at that time point, also coincided with the peak of seizure-like activity and was abolished through blockade of glutamatergic transmission or through inhibition of ictal activity [165]. Thereby, we also propose that the cell death peak observed at 14 DIV is a consequence of spontaneous, post-traumatic epileptiform discharges that begins to occur at this time [165]. With the exception of DG region, both PI uptake and SBDP 145 expression decreased at 21 DIV. The decrease of cell

death at 21 DIV could be related to the increase of anti-apoptotic cell death signaling induced by TNFR2 (see discussion of inflammatory cytokines). Over-expression and cleavage of caspase-3 have been found in hippocampal tissue from TLE patients [111,120]. But surprisingly, no expression of SBDP 120 and caspase-3 active form were obtained at any of the three time points analyzed. There is evidence of a cross-talk between the calpain and the caspase pathways, in which calpain acts upstream caspases. This means that calpain is able to cleave caspase-3, as well as other caspases at non-canonical sites, inhibiting and inactivating this caspase [196]. This may be a potential explanation for the non-activation of caspase-3 in OHSC. Fujiwaka's group also did not detect any expression of caspase-3 active form in a status epilepticus model [197]. Other researchers have shown the activation of caspase-3 only several days or even a week after status epilepticus in animal models [198,199]. The caspase-3 takes part in caspase-dependent apoptotic pathways, while calpain is involved in both necrosis and apoptosis [176]. Thereby, cell death seems mainly to occur either through necrosis and/or through the caspase-independent apoptosis pathway, being both cell death processes linked to excitotoxicity [124].

5.3 Astrogliosis and microglia activation

Experimental evidence of glia-mediated excitation and inflammation, in promoting the precipitation and the recurrence of seizures, has risen during the last decade [48,200,201]. In the OHSC model of epileptogenesis a tendency for increased GFAP protein expression was observed throughout time. IF assay demonstrated a scar-like layer formation over the slice, resembling Coltman's group description [184]. This glial scar is essential for spatial and temporal restriction of inflammation and damaged tissue and it is mainly formed by reactive astrocytes [13,202]. In our study, at 7 DIV this scar was evident in DG and CA3, while in CA1 it peaked at 14 DIV. Since mossy fiber sprouting induces an excitatory feedback network [16,23,24,136], we suggest that it is likely to be the cause of the scar appearance at DG region. Also, the scar formation in CA1 subfield at 14 DIV slices coincided with the highest neuronal loss in OHSC and, as a matter of fact, denser astrogliosis was already described to be associated with regions where prominent neuronal death occurs [45]. A profound "reorganization of glia" was described in organotypic cultures due to the trauma of culturing, in which these cells suffer a change in morphology, function and proliferation [203]. Additionally, At 21 DIV the astrocytic scar covers all regions of the hippocampus.

Regarding microglia activation, Iba-1 expression shows a decrease of about 40% at 14 and 21 DIV slices when compared to slices with 7 DIV. This decrease was also possible to be

demonstrated in the whole hippocampus images obtained through IF assay. Moreover, the activated state of microglia was observed in CA1 and CA3 regions at 7 DIV, while this state was only obtained at 14 DIV slices in DG region. In slices with 21 DIV, the microglia regains its resting state. According to the literature, this activated state remains during the first week of culture and coincides with the cell death caused by the culturing process [204,205]. Microglia converts to an active amoeboid morphology and acts as phagocytic cells in order to clear the debris of damaged cells which resulted from culturing [206]. Therefore, the functions of microglia in OHSC seem to be essential in the regulation of the degenerative responses resulted from the trauma of culturing, which is important for synaptic reorganization and repair [207].

5.4 Inflammatory mediators

Cytokines are quickly overexpressed followed CNS insults (e.g., seizures) [27] and, consequently, these inflammatory mediators alter neuronal excitability and decrease the seizures threshold, contributing to epileptogenesis (Foresti, Arisi, & Shapiro, 2010) [37]. However, the specific mechanisms by which seizure activity induces cytokine production and release in glia cells are still unclear. Cytokines can also induce excitotoxicity and apoptotic neuronal death [47,89,90]. This suggests that the release of cytokines by glia cells during seizures may contribute to seizure-mediated neuronal damage [52]. This hypothesis is supported by several evidences. For example, in respect to glutamate, IL-1β and TNF-α inhibit the astrocytic glutamate reuptake, subsequently leading to increased glutamatergic neurotransmission [53,208]. These two cytokines can also contribute to neuronal excitability through alterations in glutamate ionic receptor (AMPA) subunit expression [209], turning this receptor calcium permeable [210,211]. As a matter of fact, the IL-1β and TNF-α effect on the exacerbation in excitotoxic neuronal damage, induced by AMPA, was already demonstrated in OHSC [212]. Regarding NMDA receptors, IL-1β enhances calcium influx into neurons through these glutamate receptors [213,214]. In addition, IL-1β and TNF-α reduce the GABA-mediated inhibition through a decrease in chloride currents mediated by this neurotransmitter or by a modification in $GABA_A$ receptor [27,215,216]. Moreover, TNF-α decreases $GABA_A$-mediated inhibitory synaptic strength, inducing endocytosis of $GABA_A$ receptors [217,218]. TNF-α signaling represents the major mechanism of apoptotic cell death [30]. A constitutive expression of TNF death receptors in both astrocytes and microglia in human TLE was already documented [219,220]. It is important to highlight that cytokines effects on threshold frequency and duration of seizures are independent of cell death [211].

The OHSC model of epileptogenesis is not an exception and an increase of transcript expression of the principal cytokines associated with neuroinflammation events in epilepsy, such as the IL-1β, IL-6 and TNF-α [49,92], was observed throughout time in culture. However, significant differences were only achieved in 21 DIV slices when compared to 7 DIV slices. The mRNA expression of IL-6 did not increase throughout time, only reached a peak at 21 DIV. Since excitotoxicity is a potent inducer of IL-6 expression [116], IL-6 upregulation might be related with the induction of excitotoxicity, through IL-1β and TNF-α effects on glutamate and GABA neurotransmission. IL-6 has probably a neuroprotective effect in 21 DIV slices, diminishing the neuronal damage that was obtained at that time point [116]. Concerning the receptor's transcript expression, a significant upregulation was also solely achieved in slices with 21 DIV for IL-1RI, TNFR2 and for IL-6R. Studies using animal models of epilepsy, revealed a neuroprotective effect of TNF-α, mainly through the binding to TNFR2 [114,221], which indicates that TNF-α could be playing a role against cell damage at 21 DIV. Thus, this result may also explain the decrease of cell death obtained at this time point. IL-1β receptor type I transcript expression is significantly increased at 21 DIV slices, which is in agreement with the upregulation of the IL-1β /IL-1RI described in experimental models of TLE during epileptogenesis [11,51].

The protein expression evaluation of each cytokine was also attempted in this project. However the antibodies used (antibody against TNF-α from NovusBio (1:200) and antibody against IL-1β from Abcam (1:200)) in the western blot assays were very unspecific. For this reason, ELISA assays to evaluate study the amount of protein, in tissue and culture supernatant, are already in course. Also, IL-1β and TNF-α expression in glial cells was also attempted through immunohistochemistry assay. Double-staining of organotypic slices with GFAP/Iba1 and IL-1β show an exclusive expression of this cytokine in astrocytes at 21 DIV (**Figure 11** in Appendix section 9.5). These results are in accordance with other epileptogenesis models, in which a quick enhance of IL-1β was detected in both activated microglia and astrocytes, during acute seizures [104]. After seizure decrease, IL-1β expression did not return to the basal level and it persisted during epileptogenesis and in chronic epileptic tissue, being expressed in astrocytes and not in microglia [103,104]. These findings indicate that microglia act mostly as a source of cytokines at the onset of seizures, while astrocytes seem to be involved in the perpetuation of inflammation [104]. These features were already confirmed in human TLE tissue [51]. In fact, in contrast to astrocytes, microglia are extremely sensitive and quickly respond to small changes in the CNS [81] and microglia-secreted cytokines have been suggested to contribute to the

subsequent activation of astrocytes [222]. In summary, astrogliosis and microglia activation occurs at a different stage [51,223], like was observed in our model of epileptogenesis.

6 CONCLUSION AND FUTURE PERSPECTIVES

Our results point to an activity dependent inflammation progress, since at 21 DIV, when slices depict mixed interictal and ictal-like discharges, a significant upregulation of inflammatory mediators was observed in the OHSC model of epileptogenesis. Moreover, at 21 DIV only astrogliosis was found, while microglia reversed from an active amoeboid state to a resting state throughout time. Therefore, our data point to astrocytes as the major glial cells involved in the progression of the inflammatory process in this model. In fact, it has been reported that astrogliosis is an underlying component of the neuropathology of epilepsy [224,225]. Moreover, several studies demonstrated that microglia activation precedes astrogliosis and it is involved in its onset, which is in accordance with our results [226]. Altogether, the OHSC model of epileptogenesis can be considered a useful and simple model to decipher the specific roles and functions of glial cells and inflammation in epileptogenesis, seizure initiation and seizure spread.

In the future, we would like to better characterize the expression of IL-1β, IL-6 and TNF-α. We aim to evaluate total protein expression and release by ELISA assays, and further disclosure their expression in each cell type, by immunofluorescence assays. The pattern of expression of cytokine receptors is also important to determine the target cells of the cytokines' effects [39]. A study of anti-inflammatory cytokines will also be conducted, since the balance between pro- and anti-inflammatory cytokines is crucial for the development of inflammation [30].

The reduction of seizures through some anti-inflammatory treatments was already demonstrated in both experimental models and in clinical cases [34,45]. This model will be used to explore the effects, upon epileptogenesis, of targeting specific inflammatory pathways. With these studies we hope to provide new insights into the mechanisms of epileptogenesis and its interplay with inflammatory events and ultimately, contribute to novel pharmacologic strategies to arrest epilepsy onset and/or progression.

7 REFERENCES

1. Zigmond M., Bloom FE, Landis S, Roberts JL, Squire L. *Fundamental Neuroscience*. Academic Press. 1999.

2. Dumoulin A, Rostaing P, Bedet C, Lévi S, Isambert MF, Henry JP, Triller A, Gasnier B. Presence of the vesicular inhibitory amino acid transporter in GABAergic and glycinergic synaptic terminal boutons. *J Cell Sci*. 1999;112

3. Hirtz D, Thurman D. J, Gwinn-Hardy K., Mohamed M, Chaudhuri AR, Zalutsky R. How common are the "common" neurologic disorders? *Neurology*. 2007;68(5):326-37.

4. Thurman DJ, Beghi E, Begley CE, Berg AT, Buchhalter JR, Ding D, Hesdorffer DC, Hauser WA, Kazis L, Kobau R, Kroner B, Labiner D, Liow K, Logroscino G, Medina MT, Newton CR, Parko K, Paschal A, Preux P-M, Sander JW, Selassie A, Theodore W, Tomson T, Wiebe S. Standards for epidemiologic studies and surveillance of epilepsy. *Epilepsia*. 2011;52 Suppl 7(1):2-26.

5. Fisher RS, van Emde Boas W, Blume W, Elger C, Genton P, Lee P, Engel JJr. Epileptic Seizures and Epilepsy: Definitions Proposed by the International League Against Epilepsy (ILAE) and the International Bureau for Epilepsy (IBE). *Epilepsia*. 2005;46(10):1698-9.

6. DeLorenzo RJ, Sun DA, Deshpande LS. Cellular mechanisms underlying acquired epilepsy: The calcium hypothesis of the induction and maintainance of epilepsy. *Pharmacol Ther*. 2005;105(3):1-69.

7. Chang BS, Lowenstein DH. Epilepsy. *N Engl J Med*. 2003: 349:1257-66.

8. Engel J, Wiebe S, French J, Sperling M, Williamson P, Spencer D, Gumnit R, Zahn C, Westbrook E, Enos B. Practice parameter: temporal lobe and localized neocortical resections for epilepsy. *Epilepsia*. 2003;44(6):741-51.

9. Eadie M. Shortcoming in the current treatment of epilepsy. *Expert Rev Neurother*. 2012;12(12):1419-27

10. Binder DK, Auser CS, Words KEY. Functional Changes in Astroglial Cells in Epilepsy. *GLIA*. 2006;368:358-368.

11. Pitkänen A, Sutula TP. Is epilepsy a progressive disorder ? Prospects for new therapeutic approaches in temporal-lobe epilepsy. *Lancet Neurol.* 2002;1(7):173-181.

12. Friedman A, Dingledine R. Molecular cascades that mediate the influence of inflammation on epilepsy. *Epilepsia*. 2011;52:33-39.

13. Devinsky O, Vezzani A, Najjar S, De Lanerolle NC, Rogawski MA. Glia and epilepsy: excitability and inflammation. *Trends Neurosci*. 2013;36(3):174-84.

14. Green JD. THE HIPPOCAMPUS. *Physiol Rev*. 1964;44:561-608.

15. Sloviter RS. The neurobiology of temporal lobe epilepsy: too much information, not enough knowledge. *C R Bio*l. 2005;328(2):143-53.

16. Engel J. Mesial Temporal Lobe Epilepsy: What Have We Learned? *Neurosci*. 2001;7(4):340-352.

17. Da Silva FL. Epileptogénese. In: *Livro Básico Da EPILEPSIA* (Alves D, Luzeiro I, Pimentel J). Bial. 2007;27-64

18. Blümcke I, Thom M, Aronica E, Armstrong DD, Bartolomei F, Bernasconi A, Bernasconi, N, Bien CG, Cendes F, Coras R, Cross JH, Jacques TS, Kahane P, Mathern GW, Miyata H, Moshé SL, Oz B, Özkara Ç, Perucca E, Sisodiya S, Wiebe S, Spreafico R. International consensus classification of hippocampal sclerosis in temporal lobe epilepsy: a Task Force report from the ILAE Commission on Diagnostic Methods. *Epilepsia*. 2013;54(7):1315-29.

19. De Lanerolle NC, Noebels JL. Histopathology of Human Epilepsy. In: *Jasper's basic mechanisms of the epilepsies: histopathology of human epilepsy* (Noebels JL, Avoli M). Oxford University Press. 2012;30:387-389

20. Okazaki MM, Evenson DA, Nadler JV. Hippocampal mossy fiber sprouting and synapse formation after status epilepticus in rats: visualization after retrograde transport of biocytin. *J Comp Neurol*. 1995;352(4):515-34.

21. Represa A, Jorquera I, Le Gal La Salle G, Ben-Ari Y. Epilepsy induced collateral sprouting of hippocampal mossy fibers: does it induce the development of ectopic synapses with granule cell dendrites? *Hippocampus*. 1993;3(3):257-68.

22. Sutula T, He XX, Cavazos J, Scott G. Synaptic reorganization in the hippocampus induced by abnormal functional activity. *Science*. 1988;239(4844):1147-50.

23. Scharfman HE, Sollas AL, Berger RE, Goodman JH. Electrophysiological evidence of monosynaptic excitatory transmission between granule cells after seizure-induced mossy fiber sprouting. *J Neurophysiol*. 2003;90(4):2536-47.

24. Sharma AK, Reams RY, Jordan WH, Miller M a, Thacker HL, Snyder PW. Mesial temporal lobe epilepsy: pathogenesis, induced rodent models and lesions. *Toxicol Pathol*. 2007;35(7):984-99.

25. White H. Animal models of epileptogenesis. *Neurology*. 2002;59(9 Suppl 5):S7-S14.

26. Babb TL, Pretorius JK. Pathological substrates in epilepsy. In: *The Treatment of Epilepsy* (ER W). Philadelphia: Lea and Febiger. 1993;55-70.

27. Vezzani A, French J, Bartfai T, Baram TZ. The role of inflammation in epilepsy. *Nat Rev Neurol*. 2011;7(1):31-40.

28. Vezzani A, Rüegg S. The pivotal role of immunity and inflammatory processes in epilepsy is increasingly recognized: introduction. *Epilepsia*. 2011;52 Suppl 3:1-4.

29. Block ML, Hong JS. Microglia and inflammation-mediated neurodegeneration: Multiple triggers with a common mechanism. *Prog Neurobiol*. 2005;76(2):77-98.

30. Aloisi F. Immune Function of Microglia. *Glia.* 2001;179:165-179.

31. Ransohoff RM, Brown MA. Innate immunity in the central nervous system. *J Clin Invest*. 2012;122(4):1164-71.

32. Das M, Mohapatra S, Mohapatra SS. New perspectives on central and peripheral immune responses to acute traumatic brain injury. *J Neuroinflammation*. 2012;9:236

33. Minghetti L. Role of inflammation in neurodegenerative diseases. *Curr Opin Neurol*. 2005;18(3):315-21.

34. Vezzani A, Granata T. Brain Inflammation in Epilepsy: Experimental and Clinical Evidence, Brain Inflammation in Epilepsy: Experimental and Clinical Evidence. *Epilepsia*. 2005;46(11):1724-43.

35. Cappellano G, Carecchio M, Fleetwood T, Magistrelli L, Cantello R, Dianzani U, Comi C, Immunity and inflammation in neurodegenerative diseases. *Am J Neurodegener Dis*. 2013;2(2):89-107.

36. Glass CK, Saijo K, Winner B, Marchetto MC, Gage FH. Mechanisms underlying inflammation in neurodegeneration. *Cell*. 2010;140(6):918-34.

37. Harry GJ, Kraft AD. Neuroinflammation and Microglia: Considerations and approaches for neurotoxicity assessment. *Expert Opin Drug Metab Toxicol*. 2008;4(10):1265-1277.

38. Allan SM, Rothwell NJ. Inflammation in central nervous system injury. *Philos Trans R Soc Lond B Biol Sci*. 2003;358(1438):1669-77.

39. Vezzani A, Friedman A, Dingledine RJ. The role of inflammation in epileptogenesis. *Neuropharmacology*. 2012;69:16-24.

40. Vezzani A. Epilepsy and inflammation in the brain: overview and pathophysiology. *Epilepsy Curr*. 2014;14(1 Suppl):3-7.

41. Streit WJ, Walter SA, Pennell NA. Reactive microgliosis. *Prog Neurobiol*. 1999;57(6):563-81.

42. Shapiro L a., Perez ZD, Foresti ML, Arisi GM, Ribak CE. Morphological and ultrastructural features of Iba1-immunolabeled microglial cells in the hippocampal dentate gyrus. *Brain Res*. 2009;1266:29-36.

43. Hüttmann K, Sadgrove M, Wallraff A, Hinterkeuser S, Kirchhoff F, Steinhäuser C, Gray WP. Seizures preferentially stimulate proliferation of radial glia-like astrocytes in the adult dentate gyrus: functional and immunocytochemical analysis. *Eur J Neurosci*. 2003;18(10):2769-78.

44. Dambach H, Hinkerohe D, Prochnow N, et al. Glia and epilepsy: experimental investigation of antiepileptic drugs in an astroglia/microglia co-culture model of inflammation. *Epilepsia*. 2014;55(1):184-92.

45. Aronica E, Crino PB. Inflammation in epilepsy: clinical observations. *Epilepsia*. 2011;52 Suppl 3:26-32.

46. Nguyen MD, Julien J-P, Rivest S. Innate immunity: the missing link in neuroprotection and neurodegeneration? *Nat Rev Neurosci*. 2002;3(3):216-27.

47. Allan SM, Rothwell NJ. Cytokines and acute neurodegeneration. *Nat Rev Neurosci*. 2001;2(10):734-44.

48. Vezzani A, Ravizza T, Balosso S, Aronica E. Glia as a source of cytokines: implications for neuronal excitability and survival. *Epilepsia*. 2008;49 Suppl 2:24-32.

49. De Simoni MG, Perego C, Ravizza T, Moneta D, Conti M, Marchesi F, De Luigi A, Garattini S, Vezzani A. Inflammatory cytokines and related genes are induced in the rat hippocampus by limbic status epilepticus. *Eur J Neurosci*. 2000;12(7):2623-2633.

50. Dhote F, Peinnequin A, Carpentier P, Baille V, Delacour C, Foquin A, Lallement G, Dorandeu F. Prolonged inflammatory gene response following soman-induced seizures in mice. *Toxicology*. 2007;238(2-3):166-76.

51. Ravizza T, Gagliardi B, Noe F, Boer K, Aronica E, Vezzani A. Innate and adaptive immunity during epileptogenesis and spontaneous seizures: evidence from experimental models and human temporal lobe epilepsy. *Neurobiol Dis*. 2008;29(1):142-160.

52. Vezzani A, Balosso S, Ravizza T. The role of cytokines in the pathophysiology of epilepsy. *Brain Behav Immun*. 2008;22(6):797-803.

53. Vezzani A, Aronica E, Mazarati A, Pittman QJ. Epilepsy and brain inflammation. *Exp Neurol*. 2013;244:11-21.

54. Touzani O, Boutin H, Chuquet J, Rothwell N. Potential mechanisms of interleukin-1 involvement in cerebral ischaemia. *J Neuroimmunol*. 1999;100:203–215.

55. Saito K, Suyama K, Nishida K, Sei Y, Basile AS. Early increases in TNF-alpha, IL-6 and IL-1 beta levels following transient cerebral ischemia in gerbil brain. *Neurosci Lett*. 1996;206(2-3):149-52.

56. Vezzani A, Auvin S, Ravizza T, Aronica E. Glia-neuronal interactions in ictogenesis and epileptogenesis : role of inflammatory mediators. In: *Jasper's Basic Mechanisms of the Epilepsies* (Noebels JL, Avoli M, Rogawski MA, Olsen RW, Delgado-Escueta AV). Oxford University Press. 2012.

57. Kettenmann H, Ransom BR. *Neuroglia*. Oxford University Press. 2013.

58. Foresti ML, Arisi GM, Shapiro LA. Role of glia in epilepsy-associated neuropathology, neuroinflammation and neurogenesis. *Brain Res Rev*. 2010;66(1-2):115-122.

59. Araque A, Parpura V, Sanzgiri RP, Haydon PG. Tripartite synapses: glia, the unacknowledged partner. *Trends Neurosci*. 1999;22(5):208-15.

60. Perea G, Navarrete M, Araque A. Tripartite synapses: astrocytes process and control synaptic information. *Trends Neurosci*. 2009;32(8):421-31.

61. Nicholls D, Attwell D. The release and uptake of excitatory amino acids. *Trends Pharmacol Sci*. 1990;11(11):462-468.

62. Mennerick S, Zorumski CF. Glial contributions to excitatory neurotransmission in cultured hippocampal cells. *Nature*. 1994;368(6466):59-62.

63. Allaman I, Bélanger M, Magistretti PJ. Astrocyte-neuron metabolic relationships: for better and for worse. *Trends Neurosci*. 2011;34(2):76-87.

64. Barres BA. The Mystery and Magic of Glia: A Perspective on Their Roles in Health and Disease. *Neuron*. 2008;60(3):430-440.

65. Choi SS, Lee HJ, Lim I, Satoh JI, Kim SU. Human astrocytes: secretome profiles of cytokines and chemokines. *PLoS One*. 2014;9(4):e92325.

66. Pekny M, Nilsson M. Astrocyte activation and reactive gliosis. *Glia*. 2005;50(4):427-34.

67. Sofroniew M V. Molecular dissection of reactive astrogliosis and glial scar formation. *Trends Neurosci*. 2009;32(12):638-47.

68. Lawson LJ, Perry VH, Dri P, Gordon S. Heterogeneity in the distribution and morphology of microglia in the normal adult mouse brain. *Neuroscience*. 1990;39(1):151-70.

69. Dardiotis E, Karanikas V, Paterakis K. Traumatic Brain Injury and Inflammation : Emerging Role of Innate and Adaptive Immunity In: *Brain Injury - Pathogenesis, Monitoring, Recovery and Management* (Agrawal A). InTech. 2012;2

70. Streit WJ, Mrak RE, Griffin WST. Microglia and neuroinflammation: a pathological perspective. *J Neuroinflammation*. 2004;1(1):14.

71. Streit WJ. Microglial senescence: does the brain's immune system have an expiration date? *Trends Neurosci*. 2006;29(9):506-10.

72. Vilhardt F. Microglia: phagocyte and glia cell. *Int J Biochem Cell Biol*. 2005;37(1):17-21.

73. Färber K, Kettenmann H. Physiology of microglial cells. *Brain Res Brain Res Rev*. 2005;48(2):133-43.

74. Dilger RN, Johnson RW. Aging, microglial cell priming, and the discordant central inflammatory response to signals from the peripheral immune system. *J Leukoc Biol*. 2008;84(4):932-9.

75. Walter L, Neumann H. Role of microglia in neuronal degeneration and regeneration. *Semin Immunopathol*. 2009;31(4):513-25.

76. Loane DJ, Byrnes KR. Role of Microglia in Neurotrauma. *Neurotherapeutics*. 2010;7(4):366-377.

77. Dissing-Olesen L, Ladeby R, Nielsen HH, Toft-Hansen H, Dalmau I, Finsen B. Axonal lesion-induced microglial proliferation and microglial cluster formation in the mouse. *Neuroscience*. 2007;149(1):112-22.

78. Farina C, Aloisi F, Meinl E. Astrocytes are active players in cerebral innate immunity. *Trends Immuno*. 2007;28(3).

79. Seifert G, Carmignoto G, Steinhäuser C. Astrocyte dysfunction in epilepsy. *Brain Res Rev*. 2010;63(1-2):212-21.

80. Aronica E, Ravizza T, Zurolo E, Vezzani A. Astrocyte immune responses in epilepsy. *Glia*. 2012;60(8):1258-68.

81. Farrar, M. J., Bernstein, I. M., Schlafer, D. H., Cleland, T. A., Fetcho, J. R., & Schaffer, C. B.. Chronic in vivo imaging in the mouse spinal cord using an implanted chamber. *Nature Methods*. 2012;9(3), 297–302.

82. Sofroniew M V, Vinters H V. Astrocytes: biology and pathology. *Acta Neuropathol*. 2010;119(1):7-35.

83. Bardehle S, Krüger M, Buggenthin F, Chwausch J, Ninkovic J, Clevers H, Snippert HJ, Theis FJ, Meyer-Luehmann M, Bechmann I, Dimou L, Götz M. Live imaging of astrocyte responses to acute injury reveals selective juxtavascular proliferation. Nat Neurosci. 2013;16(5):580-6.

84. Binder DK, Steinhäuser C. Functional changes in astroglial cells in epilepsy. *Glia*. 2006;54(5):358-68.

85. Seifert G, Schilling K, Steinhäuser C. Astrocyte dysfunction in neurological disorders: a molecular perspective. *Nat Rev Neurosci*. 2006;7(3):194-206.

86. Wetherington J, Serrano G, Dingledine R. Astrocytes in the Epileptic Brain. *Neuron*. 2008;58(2):168-178. doi:10.1016/j.neuron.2008.04.002.

87. Bachstetter AD, Van Eldik LJ. The p38 MAP Kinase Family as Regulators of Proinflammatory Cytokine Production in Degenerative Diseases of the CNS. *Aging Dis*. 2010;1(3):199-211.

88. O'Neill LA., Kaltschmidt C. NF-kB: a crucial transcription factor for glial and neuronal cell function. *Trends Neurosci*. 1997;20(6):252-258.

89. Bachstetter AD, Xing B, de Almeida L, Dimayuga ER, Watterson DM, Van Eldik LJ. Microglial p38α MAPK is a key regulator of proinflammatory cytokine up-regulation induced by toll-like receptor (TLR) ligands or beta-amyloid (Aβ). *J Neuroinflammation*. 2011;8(1):79.

90. Allan SM, Tyrrell PJ, Rothwell NJ. Interleukin-1 and neuronal injury. *Nat Rev Immunol*. 2005;5(8):629-40.

91. Watkins JC, Evans RH. Excitatory amino acid transmitters. In: Okun R. *Annual Review of Pharmacology and Toxicology*. Annual Reviews; 1981:165–204.

92. Andrzejczak D. Epilepsy and pro-inflammatory cytokines. Immunomodulating properties of antiepileptic drugs.. *Neurol Neurochir Pol*. 2011;45(3):275-285.

93. Minami M, Kuraishi Y, Satoh M. Effects of kainic acid on messenger RNA levels of IL-1 beta, IL-6, TNF alpha and LIF in the rat brain. *Biochem Biophys Res Commun*. 1991;176(2):593-8.

94. Voutsinos-Porche B, Koning E, Kaplan H, Ferrandon A, Guenounou M, Nehlig A, Motte J. Temporal patterns of the cerebral inflammatory response in the rat lithium-pilocarpine model of temporal lobe epilepsy. *Neurobiol Dis*. 2004;17(3):385-402.

95. Jankowsky JL, Patterson PH. The role of cytokines and growth factors in seizures and their sequelae. *Prog Neurobiol*. 2001;63(2):125-49.

96. Dinarello CA. Biologic basis for interleukin-1 in disease. *Blood*. 1996;87(6):2095-147.

97. Rothewell NJ, Loddick SA, Stroemer P. Interleukins and Cerebral Ischaemia. In: *Neuroprotective Agents and Cerebral Ischaemia* (Green AR, Cross AJ). Academic Press. 1996;26

98. Li G, Bauer S, Nowak M, Norwood B, Tackenberg B, Rosenow F, Knake S, Oertel WH, Hamer HM. Cytokines and epilepsy. *Seizure*. 2011;20(3):249-56.

99. Curfs J, Meis J, Hoogkamp-Korstanje J. A primer on cytokines: sources, receptors, effects, and inducers. *Clin Microbiol Rev*. 1997;10(4):742-780.

100. Boutin H, Kimber I, Rothwell NJ, Pinteaux E. The Expanding Interleukin-1 Family and Its Receptors. *Mol Neurobiol.* 2003;27(3):239-248.

101. O'Neill LAJ. The interleukin-1 receptor/Toll-like receptor superfamily: 10 years of progress. *Immunol Rev*. 2008;226:10-8.

102. John GR, Lee SC, Song X, Rivieccio M, Brosnan CF. IL-1-regulated responses in astrocytes: relevance to injury and recovery. *Glia*. 2005;49(2):161-76.

103. Ravizza T, Vezzani A. Status epilepticus induces time-dependent neuronal and astrocytic expression of interleukin-1 receptor type I in the rat limbic system. *Neuroscience*. 2006;137(1):301-8.

104. Ravizza T, Gagliardi B, Noé F, Boer K, Aronica E, Vezzani A. Innate and adaptive immunity during epileptogenesis and spontaneous seizures: evidence from experimental models and human temporal lobe epilepsy. *Neurobiol Dis*. 2008;29(1):142-60.

105. Gatti S, Vezzani A, Bartfai T. Mechanisms of Fever and Febrile Seizures: Putative Role of the Interleukin-1 System. In: *Febrile Seizures* (Baram TZ, Shinnar S) Academic Press; 2002;169-88.

106. Vezzani A, Conti M, De Luigi A, Ravizza, T. Moneta, D, Marchesi, F, De Simoni, MG. Interleukin-1beta immunoreactivity and microglia are enhanced in the rat hippocampus by focal kainate application: functional evidence for enhancement of electrographic seizures. J Neurosci. 1999;19(12):5054-65.

107. Vezzani A, Balosso S, Maroso M, Zardoni D, Noé F, Ravizza T. ICE/caspase 1 inhibitors and IL-1beta receptor antagonists as potential therapeutics in epilepsy. *Curr Opin Investig Drugs*. 2010;11(1):43-50.

108. Cabal-Hierro L, Lazo PS. Signal transduction by tumor necrosis factor receptors. *Cell Signal*. 2012;24(6):1297-305.

109. Kärkkäinen I, Rybnikova E, Pelto-Huikko M, Huovila AP. Metalloprotease-disintegrin (ADAM) genes are widely and differentially expressed in the adult CNS. *Mol Cell Neurosci*. 2000;15(6):547-60.

110. Bastien D, Lacroix S. Cytokine pathways regulating glial and leukocyte function after spinal cord and peripheral nerve injury. *Exp Neurol*. 2014;258C:62-77.

111. Engel T, Henshall DC. Apoptosis, Bcl-2 family proteins and caspases: the ABCs of seizure-damage and epileptogenesis? *Int J Physiol Pathophysiol Pharmacol*. 2009;1(2):97-115.

112. Wilson NS, Dixit V, Ashkenazi A. Death receptor signal transducers: nodes of coordination in immune signaling networks. *Nat Immunol*. 2009;10(4):348-55.

113. Dempsey PW, Doyle SE, He JQ, Cheng G. The signaling adaptors and pathways activated by TNF superfamily. *Cytokine Growth Factor Rev*. 2003;14(3-4):193-209.

114. Balosso S, Ravizza T, Aronica E, Vezzani A. The dual role of TNF-α and its receptors in seizures. *Exp Neurol*. 2013;247:267-71.

115. Pickering M, O'Connor JJ. Pro-inflammatory cytokines and their effects in the dentate gyrus. *Prog Brain Res*. 2007;163:339-54.

116. Spooren A, Kolmus K, Laureys G, et al. Interleukin-6, a mental cytokine. *Brain Res Rev*. 2011;67(1-2):157-83.

117. Erta M, Quintana A, Hidalgo J. Interleukin-6, a major cytokine in the central nervous system. *Int J Biol Sci*. 2012;8(9):1254-66.

118. Brunello AG, Weissenberger J, Kappeler A, Vallan C, Peters M, Rose-John S, Weis J. Astrocytic Alterations in Interleukin-6/Soluble Interleukin-6 Receptor alpha Double-Transgenic Mice. *Am J Pathol*. 2000;157(5):1485-1493.

119. Romano M, Sironi M, Toniatti C, et al. Role of IL-6 and its soluble receptor in induction of chemokines and leukocyte recruitment. *Immunity*. 1997;6(3):315-25.

120. Bozzi Y, Dunleavy M, Henshall DC. Cell signaling underlying epileptic behavior. *Front Behav Neurosci*. 2011;5(August):45.

121. Fujikawa D. Neuroprotective Strategies in Status Epilepticus. In: *Status Epilepticus: Mechanisms and Management* (Wasterlain C, Treiman D). Cambridge 2006:463-481.

122. Choi DW. Glutamate neurotoxicity and diseases of the nervous system. *Neuron*. 1988;1(8):623-34.

123. Fujikawa DG. Prolonged seizures and cellular injury: understanding the connection. *Epilepsy Behav*. 2005;7 Suppl 3:S3-11.

124. Bengzon J, Mohapel P, Ekdahl CT, Lindvall O. Neuronal apoptosis after brief and prolonged seizures. *Prog Brain Res*. 2002;135:111-9.

125. Majno G, Joris I. Apoptosis, oncosis, and necrosis. An overview of cell death. *Am J Pathol*. 1995;146(1):3-15.

126. Ameisen JC. On the origin, evolution, and nature of programmed cell death: a timeline of four billion years. *Cell Death Differ*. 2002;9(4):367-93.

127. Strasser A, O'Connor L, Dixit VM. Apoptosis signaling. *Annu Rev Biochem*. 2000;69:217-45.

128. Castillo MR, Babson JR. Ca(2+)-dependent mechanisms of cell injury in cultured cortical neurons. *Neuroscience*. 1998;86(4):1133-44.

129. Orrenius S, Zhivotovsky B, Nicotera P. Regulation of cell death: the calcium-apoptosis link. *Nat Rev Mol Cell Biol*. 2003;4(7):552-65.

130. Xu C, Bailly-Maitre B, Reed JC. Endoplasmic reticulum stress: cell life and death decisions. *J Clin Invest*. 2005;115(10):2656-64.

131. Cain K, Bratton SB, Cohen GM. The Apaf-1 apoptosome: a large caspase-activating complex. *Biochimie*. 2002;84(2-3):203-14.

132. Ashkenazi A, Dixit VM. Death receptors: signaling and modulation. *Science*. 1998;281(5381):1305-8.

133. Yang E, Zha J, Jockel J, Boise LH, Thompson CB, Korsmeyer SJ. Bad, a heterodimeric partner for Bcl-XL and Bcl-2, displaces Bax and promotes cell death. *Cell*. 1995;80(2):285-91.

134. Vosler PS, Brennan CS, Chen J. Calpain-mediated signaling mechanisms in neuronal injury and neurodegeneration. *Mol Neurobiol*. 2008;38(1):78-100.

135. Engel J, Schwartzkroin PA. What Should Be Modeled? In: *Models of Seizures and Epilepsy* Pitkanen A, Schwartzkroin PP, Moshé SL. Elseveir Academic Press. 2006:1-14.

136. Blümcke I, Beck H, Lie a a, Wiestler OD. Molecular neuropathology of human mesial temporal lobe epilepsy. *Epilepsy Res*. 1999;36(2-3):205-23.

137. Najam I, Moder G, Janigro D. Mechanisms of epileptogenesis and experimental models of seizures. In: *The Treatment of Epilepsy: Principles & Practice*. Wyllie E, Gupta A, Lachhwani DK, eds. 4ª nd. Philadelphia: Lippincott Williams & Wilkins; 2006:91-101.

138. Löscher W. Animal models of epilepsy for the development of antiepileptogenic and disease-modifying drugs. A comparison of the pharmacology of kindling and post-status epilepticus models of temporal lobe epilepsy. *Epilepsy Res*. 2002;50(1-2):105-23.

139. Baush S. Organotypic Hippocampal Slice Cultures as a Model of Limbic Epileptogenesis . *In: Animal Models of Epilepsy: Methods and Innovations*. (Baraban SC, ed.). Human Press; 2009;9:183-201

140. Heinemann U, Kann O, Schuchmann S. An Overview of In Vitro Seizures Models in Acute and Organotypic Slices. In: *Models of Seizures and Epilepsy*. (Pitkänen A, Schwartzkroin PA, Moshé SL). Elsevier Academic Press; 2006;4:35-44

141. Wong M. Epilepsy in a dish: an in vitro model of epileptogenesis. *Epilepsy Curr*. 2011;11(5):153-4.

142. Gähwiler BH, Capogna M, Debanne D, McKinney R a, Thompson SM. Organotypic slice cultures: a technique has come of age. *Trends Neurosci*. 1997;20(10):471-7.

143. Thompson SM, Cai X, Dinocourt C, Nestor MW. The Use of Brain Slice Cultures for the study of Epilepsy. In: *Models of Seizures and Epilepsy* (Pitkänen A, Schwartzkroin PA, Moshé SL). Elsevier Academic Press; 2006;5:45-58.

144. Bernardino L, Balosso S, Ravizza T, et al. Inflammatory events in hippocampal slice cultures prime neuronal susceptibility to excitotoxic injury: A crucial role of P2X7 receptor-mediated IL-1β release. *J Neurochem*. 2008;106(1):271-280.

145. Noraberg J, Poulsen FR, Blaabjerg M, et al. Organotypic hippocampal slice cultures for studies of brain damage, neuroprotection and neurorepair. *Curr Drug Targets CNS Neurol Disord*. 2005;4(4):435-52. A

146. Gahwiler BH. Organotypic Monolayer Cultures of Nervous Tissue. *J Neurosci Methods*. 1981;4:329-342.

147. Stoppini L, Buchs P a, Muller D. A simple method for organotypic cultures of nervous tissue. *J Neurosci Methods*. 1991;37(2):173-82.

148. Molnár Z, Blakemore C. Lack of regional specificity for connections formed between thalamus and cortex in coculture. *Nature*. 1991;351(6326):475-7.

149. Holopainen IE. Organotypic hippocampal slice cultures: a model system to study basic cellular and molecular mechanisms of neuronal cell death, neuroprotection, and synaptic plasticity. *Neurochem Res*. 2005;30(12):1521-8.

150. Albus K, Wahab A, Heinemann U. Standard antiepileptic drugs fail to block epileptiform activity in rat organotypic hippocampal slice cultures. *Br J Pharmacol*. 2008;154(3):709-24.

151. Dailey E, Bergles E. Mossy Fiber Growth and Synaptogenesis in vitro in Rat Hippocampal Slices. *J Neurosci.*1994;14:1060-1078

152. Muller D, Buchs PA, Stoppini L. Time course of synaptic development in hippocampal organotypic cultures. *Brain Res Dev Brain Res*. 1993;71(1):93-100.

153. Pozzo Miller LD, Mahanty NK, Connor JA, Landis DM. Spontaneous pyramidal cell death in organotypic slice cultures from rat hippocampus is prevented by glutamate receptor antagonists. *Neuroscience*. 1994;63(2):471-87.

154. Mello LE, Cavalheiro EA, Tan AM, et al. Circuit mechanisms of seizures in the pilocarpine model of chronic epilepsy: cell loss and mossy fiber sprouting. *Epilepsia*. 1993;34(6):985-95.

155. Franck JE, Pokorny J, Kunkel DD, Schwartzkroin PA. Physiologic and morphologic characteristics of granule cell circuitry in human epileptic hippocampus. *Epilepsia*. 1995;36(6):543-58.

156. Zimmer J, Gähwiler BH. Cellular and connective organization of slice cultures of the rat hippocampus and fascia dentata. *J Comp neurobioloy*. 1984;228(3):32-46.

157. Zimmer J, Gähwiler BH. Growth of hippocampal mossy fibers: a lesion and coculture study of organotypic slice cultures. *J Comp Neurol*. 1987;264(1):1-13.

158. Routbort MJ, Bausch SB, McNamara JO. Seizures, cell death, and mossy fiber sprouting in kainic acid-treated organotypic hippocampal cultures. *Neuroscience*. 1999;94(3):755-65.

159. Gutiérrez R, Heinemann U. Synaptic reorganization in explanted cultures of rat hippocampus. *Brain Res*. 1999;815(3):04-16.

160. Dudek FE, Sutula TP. Epileptogenesis in the dentate gyrus: a critical perspective. *Prog Brain Res*. 2007;163(801):755-73.

161. Lindroos MM, Soini SL, Kukko-Lukjanov T-K, Korpi ER, Lovinger D, Holopainen IE. Maturation of cultured hippocampal slices results in increased excitability in granule cells. *Int J Dev Neurosci*. 2005;23(1):65-73.

162. Bausch SB, Mcnamara JO, Gafurov B, Cimarosti H, Henley JM. Synaptic Connections From Multiple Subfields Contribute to Granule Cell Hyperexcitability in Hippocampal Slice Cultures Synaptic Connections From Multiple Subfields Contribute to Granule Cell Hyperexcitability in Hippocampal Slice Cultures. *J Neurophysiol*. 2000;84:2918-2932.

163. McBain CJ, Boden P, Hill RG. Rat hippocampal slices “in vitro” display spontaneous epileptiform activity following long-term organotypic culture. *J Neurosci Methods*. 1989;27(1):35-49.

164. Dyhrfjeld-Johnsen J, Berdichevsky Y, Swiercz W, Sabolek H, Staley KJ. Interictal spikes precede ictal discharges in an organotypic hippocampal slice culture model of epileptogenesis. *J Clin Neurophysiol*. 2010;27(6):418-24.

165. Berdichevsky Y, Dzhala V, Mail M, Staley KJ. Interictal spikes, seizures and ictal cell death are not necessary for post-traumatic epileptogenesis in vitro. *Neurobiol Dis*. 2013;45(2):774-785.

166. Lein PJ, Barnhart CD, Pessah IN. Acute Hippocampal Slice Preparation and Hippocampal Slice Cultures. In: *In Vitro Neurotoxicology: An Introduction*. (Costa LG, Giordano G, Guizzetti M). Human Press. 2011;7

167. Vitaliti G, Pavone P, Mahmood F, Nunnari G, Falsaperla R. Targeting inflammation as a therapeutic strategy for drug-resistant epilepsies: An update of new immune-modulating approaches. *Hum Vaccines Immunother*. 2014;10(January 2015):868-875.

168. Manu H, Daniel, H. L. The search for circulating epilepsy biomarkers. *Biomark Med*. 2014;8:413-427.

169. Brewer GJ, Torricelli JR, Evege EK, Price PJ. Optimized survival of hippocampal neurons in B27-supplemented Neurobasal, a new serum-free medium combination. *Journal of Neuroscience and Research*. 1993;35(5):67-76

170. Gahwiler BH, Thompson S, McKinney RA, Debanne D, Robertson RT. Organotypic slice cultures of neural tissue. In: *Culturing Nerve Cells*. (Banker G, Goslin K). MIT Press. 1998.

171. Heeneman S, Deutz NE, Buurman WA. The concentrations of glutamine and ammonia in commercially available cell culture media. *J Immunol Methods*. 1993;166(1):85-91.

172. Hassell T, Gleave S, Butler M. Growth inhibition in animal cell culture. The effect of lactate and ammonia. *Appl Biochem Biotechnol*. 1991;30(1):29-41.

173. Macklis JD, Madison RD. Progressive incorporation of propidium iodide in cultured mouse neurons correlates with declining electrophysiological status: a fluorescence scale of membrane integrity. *J Neurosci Methods*. 1990;31(1):43-6.

174. Weiss ES, Wang KKW, Allen JG, Blue, Mary E, Nwakanma LU, Liu MC, Lange MS, Berrong J, Wilson MA, Gott VL, Troncoso JC, Ronald L, Johnston MV, Baumgartner WA. Alpha II-spectrin Breakdown Products Serve as Novel Markers of Brain Injury Severity in a Canine Model of Hypothermic Circulatory Arrest. *Ann Thorac Surg*. 2009;88(2):543-550.

175. Yan X-X, Jeromin A. Spectrin Breakdown Products (SBDPs) as Potential Biomarkers for Neurodegenerative Diseases. *Curr Transl Geriatr Exp Gerontol Rep*. 2013;1(2):85-93.

176. Wang KK. Calpain and caspase: can you tell the difference? *Trends Neurosci*. 2000;23(1):20-6.

177. Pike BR, Flint J, Dutta S, Johnson E, Wang KK, Hayes RL. Accumulation of non-erythroid alpha II-spectrin and calpain-cleaved alpha II-spectrin breakdown products in cerebrospinal fluid after traumatic brain injury in rats. *J Neurochem*. 2001;78(6):1297-306.

178. Pike BR, Flint J, Dave JR, et al. Accumulation of calpain and caspase-3 proteolytic fragments of brain-derived alphaII-spectrin in cerebral spinal fluid after middle cerebral artery occlusion in rats. *J Cereb Blood Flow Metab*. 2004;24(1):98-106.

179. Jerónimo-Santos A, Vaz SH, Parreira S, et al. Dysregulation of TrkB Receptors and BDNF Function by Amyloid-β Peptide is Mediated by Calpain. *Cereb Cortex*. 2014.

180. Eng LF, Ghirnikar RS. GFAP and astrogliosis. *Brain Pathol*. 1994;4(3):229-37.

181. Imai Y, Kohsaka S. Intracellular signaling in M-CSF-induced microglia activation: Role of Iba1. *Glia*. 2002;40(2):164-174.

182. Ito D, Imai Y, Ohsawa K, Nakajima K, Fukuuchi Y, Kohsaka S. Microglia-specific localisation of a novel calcium binding protein, Iba1. *Brain Res Mol Brain Res*. 1998;57(1):1-9.

183. Kettenmann H, Hanisch U-K, Noda M, Verkhratsky A. Physiology of microglia. *Physiol Rev*. 2011;91(2):461-553.

184. Coltman BW, Ide CF. Temporal characterization of microglia, IL-1β-like immunoreactivity and astrocytes in the dentate gyrus of hippocampal organotypic slice cultures. *Int J Dev Neurosci*. 1996;14(6):707-719.

185. Berg AT. The natural history of mesial temporal lobe epilepsy. *Curr Opin Neurol*. 2008;21(2):173-8.

186. Williams PA, White AM, Clark S, Ferraro DJ, Swiercz W, Staley KJ, Dudek FE. Development of spontaneous recurrent seizures after kainate-induced status epilepticus. *J Neurosci*. 2009;29(7):2103-12.

187. White A, Williams PA, Hellier JL, Clark S, Dudek FE, Staley KJ. EEG spike activity precedes epilepsy after kainate-induced status epilepticus. *Epilepsia*. 2010;51(3):371-83.

188. Morrison B, Elkin BS, Dollé J-P, Yarmush ML. In Vitro Models of Traumatic Brain Injury. *Annu. Rev. Biomed. Eng*; 2011:91-126.

189. Schwartzkroin PA. Hippocampal slices in experimental and human epilepsy. *Adv Neurol*. 1986;44:991-1010.

190. Fertig EJ, Spencer SS. Hippocampal Sclerosis and Dual Pathology. In: *The Treatment of Epilepsy: Principles & Practice* .(Wyllie E, Gupta A, Lachhwani DK). Philadelphia: Lippincott Williams & Wilkins; 2006:1069-1085.

191. Czogalla A, Sikorski AF. Spectrin and calpain: a "target" and a "sniper" in the pathology of neuronal cells. *Cell Mol Life Sci*. 2005;62(17):1913-24.

192. O'Dell CM, Das A, Wallace G, Ray SK, Banik NL. Understanding the basic mechanisms underlying seizures in mesial temporal lobe epilepsy and possible therapeutic targets: a review. *J Neurosci Res*. 2012;90(5):913-24.

193. Cavazos JE, Cross DJ. The role of synaptic reorganization in mesial temporal lobe epilepsy. *Epilepsy Behav*. 2006;8(3):483-93.

194. Siman R, Noszek JC, Kegerise C. Calpain I activation is specifically related to excitatory amino acid induction of hippocampal damage. *J Neurosci*. 1989;9(5):1579-90.

195. Vornov JJ, Tasker RC, Park J. Neurotoxicity of acute glutamate transport blockade depends on coactivation of both NMDA and AMPA/Kainate receptors in organotypic hippocampal cultures. *Exp Neurol*. 1995;133(1):7-17.

196. Lankiewicz S, Marc Luetjens C, Truc Bui N, et al. Activation of calpain I converts excitotoxic neuron death into a caspase-independent cell death. *J Biol Chem*. 2000;275(22):17064-71.

197. Fujikawa DG, Ke X, Trinidad RB, Shinmei SS, Wu A. Caspase-3 is not activated in seizure-induced neuronal necrosis with internucleosomal DNA cleavage. *J Neurochem*. 2002;83(1):229-40.

198. Weise J, Engelhorn T, Dörfler A, Aker S, Bähr M, Hufnagel A. Expression time course and spatial distribution of activated caspase-3 after experimental status epilepticus: contribution of delayed neuronal cell death to seizure-induced neuronal injury. *Neurobiol Dis*. 2005;18(3):582-90.

199. Narkilahti S, Pirttila TJ, Lukasiuk K, Tuunanen J, Pitkanen A. Expression and activation of caspase 3 following status epilepticus in the rat. *Eur J Neurosci*. 2003;18(6):1486-1496.

200. Li T, Quan Lan J, Fredholm BB, Simon RP, Boison D. Adenosine dysfunction in astrogliosis: cause for seizure generation? *Neuron Glia Biol*. 2007;3(4):353-66.

201. Haydon PG, Carmignoto G. Astrocyte control of synaptic transmission and neurovascular coupling. *Physiol Rev*. 2006;86(3):1009-31.

202. Rolls A, Shechter R, Schwartz M. The bright side of the glial scar in CNS repair. *Nat Rev Neurosci*. 2009;10(March):235-241.

203. Huuskonen J, Suuronen T, Miettinen R, van Groen T, Salminen A. A refined in vitro model to study inflammatory responses in organotypic membrane culture of postnatal rat hippocampal slices. *J Neuroinflammation*. 2005;2:25.

204. Hailer NP, Heppner FL, Haas D, Nitsch R. Fluorescent dye prelabelled microglial cells migrate into organotypic hippocampal slice cultures and ramify. *Eur J Neurosci*. 1997;9(4):863-6.

205. Hailer NP, Jarhult JD, Nitsch R. Resting microglial cells in vitro: analysis of morphology and adhesion molecule expression in organotypic hippocampal slice cultures. *Glia*. 1996;18(4):319-31.

206. Stence N, Waite M, Dailey ME. Dynamics of microglial activation: a confocal time-lapse analysis in hippocampal slices. *Glia*. 2001;33(3):256-66.

207. Skibo GG, Nikonenko IR, Savchenko VL, McKanna JA. Microglia in organotypic hippocampal slice culture and effects of hypoxia: ultrastructure and lipocortin-1 immunoreactivity. *Neuroscience*. 2000;96(2):427-38.

208. Domercq M, Brambilla L, Pilati E, Marchaland J, Volterra A, Bezzi P. P2Y1 receptor-evoked glutamate exocytosis from astrocytes: control by tumor necrosis factor-alpha and prostaglandins. *J Biol Chem*. 2006;281(41):30684-30696.

209. Hu S, Sheng WS, Ehrlich LC, Peterson PK, Chao CC. Cytokine effects on glutamate uptake by human astrocytes. *Neuroimmunomodulation*. 2000;7(3):153-9.

210. Brorson JR, Manzolillo PA, Miller RJ. Ca2+ entry via AMPA/KA receptors and excitotoxicity in cultured cerebellar Purkinje cells. *J Neurosci*. 1994;14(1):187-97.

211. Vezzani A, Baram TZ. New roles for interleukin-1 bta in the mechanisms of epilepsy. *Epilepsy Curr*. 2007;7(2):45-50.

212. Bernardino L, Xapelli S, Silva AP, Jakobsen B, Poulsen FR, Oliveira CR, Vezzani A, Malva JO, Zimmer J. Modulator effects of interleukin-1beta and tumor necrosis factor-alpha on AMPA-induced excitotoxicity in mouse organotypic hippocampal slice cultures. *J Neurosci*. 2005;25(29):6734-44.

213. Viviani B, Bartesaghi S, Gardoni F, Vezzani A, Behrens MM, Bartfai T, Binaglia M, Corsini E, Di Luca M, Galli CL, Marinovich M. Interleukin-1beta enhances NMDA receptor-mediated intracellular calcium increase through activation of the Src family of kinases. *J Neurosci*. 2003;23(25):8692-700.

214. Balosso S, Maroso M, Sanchez-Alavez M, Ravizza T, Frasca A, Bartfai T, Vezzani A. A novel non-transcriptional pathway mediates the proconvulsive effects of interleukin-1beta. *Brain*. 2008;131:3256-65.

215. Vezzani A, Maroso M, Balosso S, Sanchez M-A, Bartfai T. IL-1 receptor/Toll-like receptor signaling in infection, inflammation, stress and neurodegeneration couples hyperexcitability and seizures. *Brain Behav Immun*. 2011;25(7):1281-9.

216. Viviani B, Gardoni F, Marinovich M. Cytokines and neuronal ion channels in health and disease. *Int Rev Neurobiol*. 2007;82:247-63.

217. Beattie EC, Stellwagen D, Morishita W, Bresnahan JC, Ha BK, Von Zastrow M, Beattie MS, Malenka RC. Control of synaptic strength by glial TNFalpha. *Science*. 2002;295(5563):2282-5.

218. Stellwagen D, Beattie EC, Seo JY, Malenka RC. Differential regulation of AMPA receptor and GABA receptor trafficking by tumor necrosis factor-alpha. *J Neurosci*. 2005;25(12):3219-28.

219. Dörr J, Bechmann I, Waiczies S, et al. Lack of tumor necrosis factor-related apoptosis-inducing ligand but presence of its receptors in the human brain. *J Neurosci*. 2002;22(4):RC209.

220. Bechmann I, Mor G, Nilsen J, Eliza M, Nitsch R, Naftolin F. FasL (CD95L, Apo1L) is expressed in the normal rat and human brain: evidence for the existence of an immunological brain barrier. *Glia*. 1999;27(1):62-74.

221. Weinberg MS, Blake BL, McCown TJ. Opposing actions of hippocampus TNFα receptors on limbic seizure susceptibility. *Exp Neurol*. 2013;247:429-37.

222. Zhang D, Hu X, Qian L, et al. Prostaglandin E2 released from activated microglia enhances astrocyte proliferation in vitro. *Toxicol Appl Pharmacol*. 2009;238(1):64-70.

223. Liu W, Tang Y, Feng J. Cross talk between activation of microglia and astrocytes in pathological conditions in the central nervous system. *Life Sci*. 2011;89(5-6):141-146.

224. Miyazaki T, Miyamoto O, Janjua NA, Hata T, Takahashi F, Itano T. Reactive gliosis in areas around third ventricle in association with epileptogenesis in amygdaloid-kindled rat. *Epilepsy Res*. 2003;56(1):5-15.

225. Khurgel M, Ivy GO. Astrocytes in kindling: relevance to epileptogenesis. *Epilepsy Res*. 1996;26(1):163-75.

226. Zhang D, Hu X, Qian L, O'Callaghan JP, Hong J-S. Astrogliosis in CNS Pathologies: Is There A Role for Microglia?. *Mol Neurobiol*. 2013;41(0):232-241.

227. Burnette WN. "Western blotting": electrophoretic transfer of proteins from sodium dodecyl sulfate--polyacrylamide gels to unmodified nitrocellulose and radiographic detection with antibody and radioiodinated protein A. *Anal Biochem*. 1981;112:195-203.

228. Mahmood T, Yang P-C. Western blot: technique, theory, and trouble shooting. *N Am J Med Sci*. 2012;4(9):429-34.

229. Kurien BT, Scofield RH. Western blotting. *Methods*. 2006;38(4):283-93.

230. Luttmann W, Bratke K, Kupper M, Myrtek D. *Immunology*. Academic Press. 2006.

231. Wilson K, Walker J. *Principles and Techniques of Biochemistry and Molecular Biology*. Cambridge University Press. 2010.

232. Carter M, Shieh J. *Guide to Research Techniques in Neuroscience*. Academic Press. 2009.

233. Mullis K, Faloona F, Scharf S, Saiki R, Horn G, Erlich H. Specific enzymatic amplification of DNA in vitro: the polymerase chain reaction. *Cold Spring Harb Symp Quant Biol*. 1986;51:263-73.

234. Pelt-Verkuil E van, Belkum A van, Hays JP. *Principles and Technical Aspects of PCR Amplification*. Springer Science & Business Media. 2008

235. Baltimore D. RNA-dependent DNA polymerase in virions of RNA tumour viruses. *Nature*. 1970;226(5252):1209-11.

236. Temin HM, Mizutani S. RNA-dependent DNA polymerase in virions of Rous sarcoma virus. *Nature*. 1970;226(5252):1211-3.

237. Reiter M, Pfaffl MW. RT-PCR Optimization Strategies. In: *PCR Troubleshooting and Optimization: The Essential Guide*. (Kennedy S). Caiser Academic Press; 2011;5:97-118

238. Dorak T. *Real-Time PCR (BIOS Advanced Methods)*. Taylor & Francis Group. 2006

239. VanGuilder HD, Vrana KE, Freeman WM. Twenty-five years of quantitative PCR for gene expression analysis. *Biotechniques*. 2008;44(5):619-26.

240. Brunner AM, Yakovlev IA, Strauss SH. Validating internal controls for quantitative plant gene expression studies. *BMC Plant Biol*. 2004;4:14.

241. Nolan T, Hands RE, Bustin SA. Quantification of mRNA using real-time RT-PCR. *Nat Protoc*. 2006;1(3):1559-82.

242. Pfaffl MW. A new mathematical model for relative quantification in real-time RT-PCR. *Nucleic Acids Res*. 2001;29(9):e45.

243. Thellin O, Zorzi W, Lakaye B, De Borman B, Coumans B, Hennen G, Grisar T, Igout A, Heinen, E. Housekeeping genes as internal standards: use and limits. *J Biotechnol*. 1999;75(2-3):291-5.

244. GelRed & GelGreen Nucleic Acid Gel Stains - Biotium: http://biotium.com/technology/gelred-gelgreen-nucleic-acid-gel-stains/. Accessed August 26, 2014.

245. Coons AH, Creech HJ, Jones RN. Immunological Properties of an Antibody Containing a Fluorescent Group. *Exp Biol Med*. 1941;47(2):200-202.

246. Petersen K, Pedersen HC. Detection Methods. In: *EDUCATIONAL Immunohistochemical Staining Methods.* (Taylor CR, Rudbeck L). DAKO. 2013:78-93.

247. Ramos-Vara JA. Technical aspects of immunohistochemistry. *Vet Pathol*. 2005;42(4):405-26.

248. Corley RB. *A Guide to Methods in the Biomedical Sciences*. Springer Science & Business Media. 2005:142.

249. Gratton E, VandeVen MJ. Laser Sources for Confocal Microscopy. In: *Handbook of Biological Confocal Microscopy.* (Pawley J). Springer Science & Business Media; 2010:80-118.

250. Fritschy J-M. Is my antibody-staining specific? How to deal with pitfalls of immunohistochemistry. *Eur J Neurosci*. 2008;28(12):2365-70.

251. Wittwer, C. T., & Farrar, J. S. Magic in solution: an Introduction and Brief History of PCR. In: *PCR Troubleshooting and Optimization: The Essential Guide* (S. Kennedy & N. Oswald). Caister Academic Press. 2011;1-22

8. APPENDIX

8.1 Preparation of OHSC

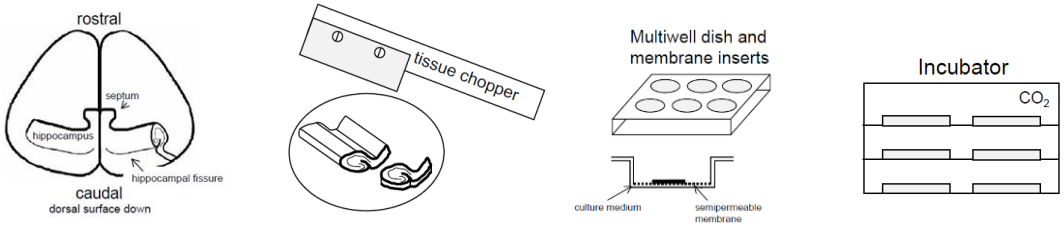

Figure 9 | Preparation of organotypic hippocampal slice cultures. First the hippocampus and part of entorhinal cortex are dissected out from the neonatal brain. The sections are sliced using a tissue chopper, under aseptic conditions, and five slices are placed on a membrane insert in a 6-multiwell dish. Cultures are maintained in a CO_2 incubator (adapted from Heinemann et al., 2006).

8.2 OHSC maintenance

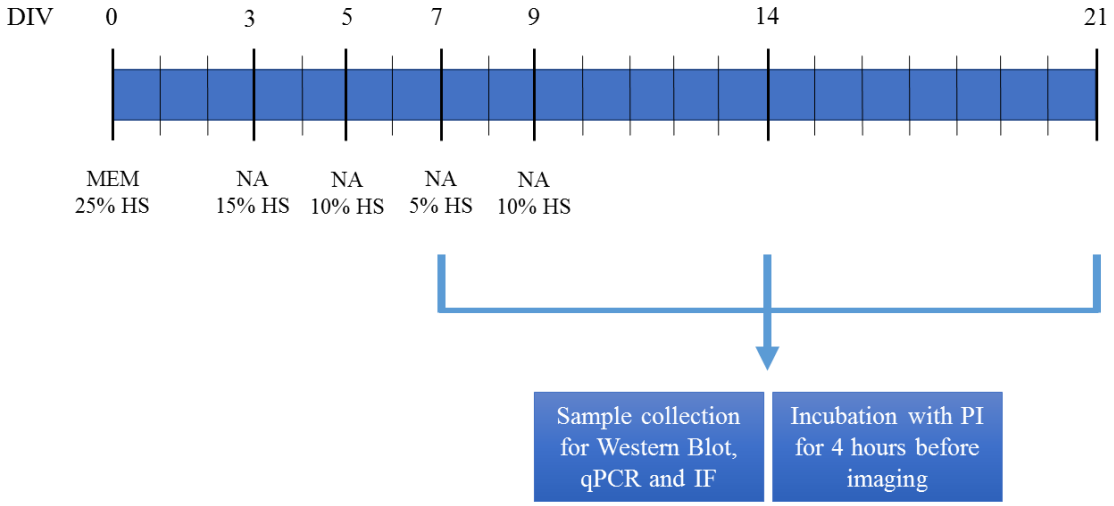

Figure 10 | Schematic representation of the OHSC maintenance. OHSCs were kept in Opti-MEM based medium with 25% of horse serum (HS) until 3 days. Started at 3 DIV, the medium was changed every second day with Neurobasal A (supplemented with 2% B27, 1mM L-glutamine and antibiotics) in the presence of decreasing concentrations of HS (15%, 10% and 5%), until complete serum-free medium was reached at 9 DIV. Slices were collected at 7, 14 and 21 DIV to perform western blot, qPCR and immunofluorescence assays. For PI assay the slices were incubated with PI solution diluted in culture medium for 4 hours before imaging. DIV, days *in vitro*; HS, horse serum; NA, Neurobasal A.

8.3 Primary antibodies

Table 1 | Primary antibodies used in Western Blot (WB)

Protein	Supplier	Host	Dilution
α-II Spectrin	Santa Cruz Biotechnology	Mouse monoclonal antibody	1:500
Caspase-3	Santa Cruz Biotechnology	Rabbit polyclonal antibody	1:1000
GFAP	Sigma	Rabbit polyclonal antibody	1:5000
Iba-1	Abcam	Goat polyclonal antibody	1:1000
GAPDH	Abcam	Mouse monoclonal antibody	1:1000

GFAP – Glial fibrillary acidic protein; **Iba-1** – Ionized calcium binding adaptor molecule 1; **GAPDH** – Glyceraldehyde-3-phosphate dehydrogenase

Table 2 | Primary antibodies used in immunohistochemistry assay

Protein	Supplier	Host	Dilution
GFAP	Sigma	Mouse monoclonal antibody	1:500
Iba-1	Abcam	Goat polyclonal antibody	1:1000
IL-1β	Abcam	Rabbit polyclonal antibody	1:100

GFAP – Glial fibrillary acidic protein; **Iba-1** – Ionized calcium binding adaptor molecule 1; **IL-1β** – Interleukin-1 beta

8.4 Primers

Table 3 | Primers used in qPCR

Gene	Primer sequence	PCR Fragment size (pb)
GAPDH	**Forward:** GTTTGTGATGGGTGTGAACC **Reverse:** TCTTCTGAGTGGCAGTGATG	170
IL-1β	**Forward:** TCCTCTGTGACTCGTGGGAT **Reverse:** GTTTGGGATCCACACTCTCCA	309
IL-1RI	**Forward:** GTCGCTGGAGACCGACAAAT **Reverse:** CAGGTCTGTCCCTCTTGCTG	635
IL-1RII	**Forward:** TCTGGAACTCAAGGTCTTTAAG **Reverse:** CTTGACCCCAAAGATGCTGGT	336
TNF-α	**Forward:** ATGGGCTCCCTCTCATCAGT **Reverse:** GCTTGGTGGTTTGCTACGAC	106
TNFR1	**Forward:** TGGCTCATGATCGGGCTTAC **Reverse:** GTAGGTTCCTTTGTGGCACT	415
TNFR2	**Forward:** CGCATTTGTAGCATCCTGGC **Reverse:** AGGCAGGAGGGCTTCTTTTT	332
IL-6	**Forward:** GCAAGAGACTTCCAGCCAGT **Reverse:** TTGCCATTGCACAACTCTTTTCT	203
IL-6R	**Forward:** TTGAAGACTATGACAACCAC **Reverse:** ATACGGTGGGGGAGAAGTCG	227

GAPDH – Glyceraldehyde-3-phosphate dehydrogenase adaptor molecule 1; **IL-1β** – Interleukin-1 beta; **IL-1RI** – Interleukin-1 receptor type I; **IL-1RII** – Interleukin 1 receptor type II; **TNF-α** – Tumor necrosis factor alpha; **TNFR1** – Tumor necrosis factor receptor type I; **TNFR2** – Tumor necrosis factor receptor type II; **IL-6** – Interleukin-6; **IL-6R** – Interleukin-6 receptor

8.5 Immunofluorescence Assays

In order to evaluate the expression of the cytokines in glial cells, immunofluorescence assays were attempted. Antibodies that recognize each cytokine and the antibodies specific for astrocytes (GFAP) and microglia (Iba-1), were used in these assays. But, unfortunately, and in spite of many attempts, only the IL-1β antibody (1:100, Abcam) worked in these assays. The next panel (**Figure 11**) shows the co-localization (yellow staining) between IL-1β and GFAP at 21 DIV slices, confirming the expression of this cytokine in astrocytes.

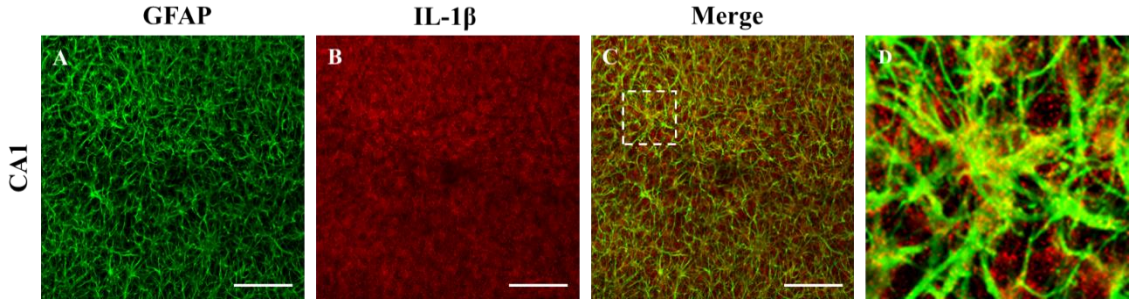

Figure 11 | Expression of IL-1β in astrocytes. Detection of GFAP stained astrocytes (green, panel A) with IL-1β (red, panel B) in CA1 region of the hippocampus, at 21 DIV slices. The last panel (D) is a magnification of the dotted region in the merge image (C) and clearly shows IL-1β expression in astrocytes. Confocal images were obtained with a 20x objective. Scale bar, 200µm.

The immunofluorescence assay carried out with IL-1β and Iba-1 antibodies is depicted in (**Figure 12**) and indicated that IL-1β was not expressed in microglia cells.

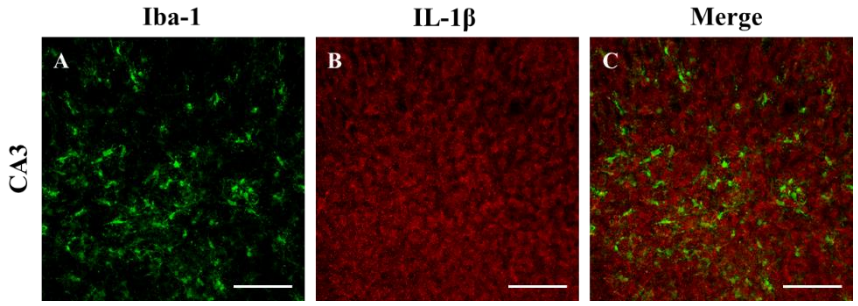

Figure 12 | Expression of IL-1β in microglia. Detection of Iba-1 stained microglia (green, panel A) with IL-1β (red, panel B) in CA3 region of the hippocampus, at 21 DIV slices. IL-1β is not expressed in microglia cells, since no overlap between IL-1β and Iba-1 can be found in the merge image (C). Confocal images were obtained with a 20x objective. Scale bar, 200µm.

8.6 Theoretical description of the experimental techniques

8.6.1 Western blot

The western blot technique (also named as the protein immunoblot) arose from the need to create a sensitive assay to detect specific proteins as well as to quantify the protein expression from a complex mixture of proteins extracted from cells or tissues. This assay is based on protein interaction with a specific antibody and its relative molecular weight. The technique's designation was given by W. Neal Burnette and is derived from the name Southern blot (the first transfer process of macromolecules from a gel to an immobilizing matrix). Antibodies can be classified as monoclonal antibodies (mAbs), which recognize a single epitope, or as polyclonal antibodies, consisting in a combination of immunoglobulin molecules, each identifying a different epitope [227].

The method involves three major steps: 1) separation of a complex protein mixture by size through gel electrophoresis, 2) protein transfer onto a membrane and 3) marking the target proteins by antibody-antigen specificity [228] .

Prior to these procedures the protein is extracted from tissues and quantified in order to ensure equal loading in all lanes of the gel. Several spectrophotometric methods are available to calculate protein concentration. Protein extraction can be achieved through homogenization or sonication, always in cold temperature, with an adequate buffer to maintain pH and in presence of protease inhibitors to prevent protein damage. The obtained lysates are diluted in a loading buffer that contains SDS, glycerol and bromophenol blue. SDS is an anionic detergent that binds to hydrophobic regions, causing the protein to acquire a net negative charge. Thus, the protein is able to move in an electric field during electrophoresis procedure, toward the positive charged electrode [229].

The most widely used method to separate protein mixtures is the sodium dodecyl sulphate-polyacrylamide gel electrophoresis (SDS-PAGE). It maintains polypeptides in a denatured state and creates a three-dimensional network, allowing proteins to be discriminated according to their molecular weight. The gel density (pore size) affects the separation profile of the proteins, since larger molecules are more retarded by the gel than the smaller ones. Samples must be previously denatured, in order to ensure that proteins are separated on the basis of size and not

charge or three-dimensional structure [229].The SDS-PAGE gel is composed by two types of acrylamide gel. Initially, protein samples run through a lower density gel, called stacking gel. This gel has lower acrylamide concentration making it highly porous, and concentrates the proteins into thin and sharply defined bands, before they enter the resolving gel. The resolving gel has higher polyacrylamide content, making gel pores narrower [230].

Subsequently, the proteins are transferred to a membrane by electroblotting, which relies on the same electromobility principles that drive the migration and separation of proteins. Membranes are typically made of chemical inert substances, such as nitrocellulose or polyvinylidene difluoride (PVDF). In order for the proteins to move from gel to membrane (blot), in a pattern that perfectly mirrors their migration positions in the gel, the membrane is placed between the gel surface and the positive electrodes in a sandwich. The membrane is immersed in transfer buffer, which provides an electrically conducting medium where proteins are soluble [228,229]. The effectiveness of transfer can be checked by staining the membrane either with Coomassie Brilliant Blue or Ponceau S dyes.

Finally, the transferred proteins can be identified by probing the blot with specific antibodies. The first step is the membrane blocking to provide a minimized background of non-specific binding between the membrane and the antibody used for detection of the target protein. This step is achieved by incubating the membrane in a protein-enriched solution (e.g., bovine serum albumin (BSA) or nonfat dried milk) in anionic detergents (e.g., TBST) [228]. Following the blocking step, the protein of interest is targeted either through a direct or indirect method system. In both methods, the antibodies have to be labeled with reporter molecules. The labels can be enzymes, fluorescent compounds and metals, that are attached to the primary or secondary antibody. The direct method is the simplest, involving one-step. The membrane is incubated with a specific primary antibody which is conjugated to the reporter molecule. The indirect labeling method involves membrane incubation with an unlabeled primary antibody and then with an enzyme conjugated secondary antibody. The secondary-Ab is directed against the IgG of the species that provided the primary antibody [231]. The most common enzymatic detection system used is based on antibodies conjugated to horseradish peroxidase (HRP). This enzyme cleaves a chemiluminescent agent, and results in light emission capable of impressing an X-ray film. The signal intensity is proportional to the protein quantity on the blot, allowing relative precise quantification. All bands are normalized to a housekeeping gene (e.g.,

Glyceraldehyde 3-phosphate dehydrogenase, α-tubulin, β-actin). Densitometric analysis of protein bands is carried out by Image J software [229,230,232].

8.6.2 qPCR

The polymerase chain reaction (PCR) is a fundamental tool in biological and medical research, used to amplify DNA sequences *in vitro*. Developed by Kary Mulis in 1983, this biochemical technology is described as a thermal cycling process that requires specific designed primers (short DNA fragments), containing sequences complementary to the target region, the four deoxyribonucleotides thrisphosphate (dNTPs), a thermostable DNA polymerase, and magnesium ions which are co-factors of DNA polymerase [233,234]. PCR amplification consists in three basic steps. Initially, the double-stranded DNA (dsDNA) is heated at a high temperature (90-95ºC for 30s to 15 min) to separate it in two single strands (denaturation step). Subsequently, the hybridization of the specific oligonucleotide primers for each DNA strand is achieved by lowering the temperature, usually between 40ºC and 70ºC (for 30-60s), depending on the composition of the primers in terms of each dNTPs. This step, designed as annealing step, is then followed by the elongation step in which DNA polymerase synthesizes a new DNA strand complementary to the DNA template strand by adding dNTPs at the optimal temperature of DNA polymerase (72ºC for 60-120s). The entire cycle is then repeated a pre-determined number of times, resulting in an exponential amplification of target molecules during each cycle. The PCR specificity depends on the correct hybridization of primer specific sequences [234].

The reverse transcriptase PCR (RT-PCR) is a variant of PCR, which turns to be the method of choice for RNA detection and quantification. Since it is more sensitive than other techniques (e.g Northen Blot, RNase protection assay), it is ideal for detecting mRNA from small amount of tissue sample [234]. RT-PCR is based on the transcription of RNA molecules into complementary DNA (cDNA) by the action of reverse transcriptase enzyme, which can then be amplified by PCR [251,234]. The discovery of an RNA-dependent DNA polymerase or reverse transcriptase was first reported during the study of viral replication by Howard Temin and then isolated by Baltimore in 1970 [235,236].

The validity and accuracy of gene expression evaluation is known to be profoundly affected by the quality of the starting RNA. It includes both RNA purity (absence of protein and DNA contamination and absence of inhibitors) and its integrity. The purity can be assessed by several

methods including spectrophotometry. RNA has its absorption maximum at 260 nm. Since proteins absorb light at 280 nm the ratio of absorptions at 260 nm and 280 nm (A_{260}/A_{280}) is commonly used to assess RNA contamination of protein solutions. There are other sources of contamination that produce peaks in the 220-230 nm region such as phenol in the RNA solution. Pure RNA has an A_{260}/A_{280} ratio of 2.1, and a A_{260}/A_{230} ratio of 2.0 [237].

Another important version of PCR is the Real-time PCR, which is the most sensitive and quantitative method. This technique integrates both detection, amplification and quantification of newly synthesized DNA through a fluorescence signal [238]. There are two main classes of detection systems: fluorescently labelled probes (standard specific detection; e.g., Taqman) and dsDNA dyes (non-specific detection; e.g., SYBR Green I) [239]. Time, temperature and fluorescence are monitored during PCR in real-time instruments [251].

Real-time PCR analysis can be absolute (number of copies of target DNA molecules) or relative (fold-differences in transcription of the target gene, based on an internal reference gene). The majority of analyses use relative quantification, since it is easier to carry out and does not require a calibration curve as the absolute analysis [239-240]. The fluorescence values are recorded during each cycle at the end of the elongation step, and the amount the fluorescence signal is directly proportional to DNA concentration. A fluorescence threshold is stipulated, known as threshold cycle (Ct) or crossing point (CP). Ct is defined as the basal level of detection at which the reaction reaches fluorescence intensity above background, in the exponential phase [241]. The higher the amount of sample DNA of a certain gene, the sooner the accumulated product is detected at the threshold level, thus, the lower the Ct value is.

In the mathematical model developed by Michael W. Pfaffl [242], the relative expression ratio of a target gene is calculate based on RT-qPCR efficiency (E) and CP deviation of a treated sample versus a control, and expressed in comparison to a reference gene (**Figure 13**). The efficiency is calculated according to [E=10^(-1/slope)], and the slope value is calculated by plotting the CP values vs. log cDNA concentration (ng/µl) from a dilution series. The CP values of each target gene are also required and are determined by subtracting the CP values in control and sample conditions for both target (ΔCPtarget) and endogenous reference (ΔCPref) genes. The normalization of the target gene expression to an endogenous reference gene ensures the compensation for inter-PCR variations between runs. Housekeeping genes are usually used, since they are expressed in all nucleated cell types and their mRNA synthesis has relatively constant levels even in different tissues and under various experimental conditions [243].

$$\text{ratio} = \frac{(E_{\text{target}})^{\Delta \text{CP}_{\text{target}}(control - sample)}}{(E_{\text{ref}})^{\Delta \text{CP}_{\text{ref}}(control - sample)}}$$

Figure 13 | Mathematical model of relative expression ratio in Real-Time PCR (qPCR) (Adapted from Pfaffl 2001)

8.6.3 Gel electrophoresis

The electrophoretic separation of nucleic acids is usually carried out in agarose gels, instead of polyacrylamide gel, since the majority of DNA molecules and their fragments are larger than proteins. Therefore, the larger pore size of an agarose gel is required for the separation of nucleic acid fragments [231]. GelRed is an intercalating nucleic acid fluorophore that, when exposed to ultraviolet light, fluoresces with an orange color. It is less toxic and more sensitive than ethidium bromide, which, in spite of being a highly mutagenic material, has been the predominant dye used for nucleic acid gel staining for decades (GelRed & GelGreen Nucleic Acid Gel Stains - Biotium). In agarose gels, as in SDS-PAGE, using an electric field, molecules (such as DNA) will run through the pores of the gel. Since DNA has a negative net charge, carried by their sugar-phosphate backbone, it will move to the positive electrode and away from the negative electrode. Several factors influence how fast the DNA moves, including the strength of the electrical field, the concentration of agarose in the gel and the size of the DNA molecules. Smaller DNA molecules move through the agarose faster than larger molecules [231].

8.6.4 Immunohistochemistry

Based on the specific capacity of antibodies (Abs), immunohistochemistry (IHC) is widely used to detect and localize cellular constituents (antigens) *in situ*, both on individual/cultured cells and in a tissue or an organism. It was developed by A. Coons and colleagues in 1941 and it is considered to be a helpful tool in the neuroscience field [245].

The interaction between antigen and Ab can be detected by either direct or indirect methods. One of the advantages of the direct method in IHC is the shorter sample staining times. Although it is not frequently used, since it produces a weak signal, it generally has high cost and low flexibility. In contrast, the indirect method has greater sensitivity. Moreover, secondary Abs are relatively inexpensive, available in an array of colors and quality controlled. The

disadvantages of this method include higher background signal and potential cross-reactivity when performing multiple-labeling experiments. To avoid this problem, Abs that are not raised in the same species or Abs of different isotypes must be used [246,247].

8.6.4.1 Immunofluorescence microscopy

Immunofluorescence (IF) microscopy uses fluorophores as reporter molecules conjugated to Abs. The specimen is submitted to a light of a specific wavelength, which is absorbed by the fluorophores (excitation) and then part of this energy is re-emitted at longer specific wavelengths (emission). Fluorescent staining can be visualized with standard fluorescent microscopy and also with confocal microscopes [246–248].

The confocal microscope focuses a spot of light onto a single point at a specific depth in the tissue. For that, it requires a very bright source of illumination, which is supplied by a laser whose light is reflected by multiple mirrors, with the objective to scan the laser across the sample. The fluorescence emitted from the illuminated material passes across a pinhole and is collected and brought to an image at a suitable light detector. Confocal microscopy not only provides information on structures in an individual plane but is also capable of collecting multiple serial optical sections from thick specimens, in the z direction generating a z-stack. Thus, through computer programs it enables the reconstruction of an optical image of the cell in a three-dimensional structure. Another advantage of this optical imaging technique is the blockage of sample fluorescence at the pinhole, eliminating the out-of-focus signals. Therefore, this increases the resolution at the cost of less signal since not all emitted light is collected. However, brighter images can be acquired in comparison to standard epifluorescence [249].

The outcome of an immunohistochemical reaction depends on the properties of the Abs used and the tissue preparation, mainly its fixation [250]. To preserve cells and tissues in reproducible and life-like manner, generally, immunostaining is carried out on fixed and permeabilized tissues (solubilize membranes) prepared by aldehydes (e.g., paraformaldehyde or formaldehyde). Further permeabilization can be accomplished with a detergent, such as Triton X-100, in order to guarantee that Abs are able to access the intracellular antigens. Subsequently, the tissue is incubated with a blocking solution, thus avoiding non-specific protein binding sites (e.g., BSA, powder milk). The following steps involve the incubation of primary and secondary Ab (coupled with a fluorophore). The multiple immunolabeling depends on whenever the primary Abs are produced in the same species (sequential dual labelling is performed) or in

different species (tissue can be incubated simultaneously with both Abs). In this way, the false positive staining is avoided. The false negatives must also be assessed to evade problems of the specificity of an antibody [231,248,248]. The last step consists in mounting the samples, in order to protect the tissue and avoid the quenching of fluorescence.

8.7 qPCR primer specificity

8.7.1 Standard and melting curve analysis

The following figures illustrate the qPCR standard and melting curves for each analyzed gene. For the analysis of the transcript expression, 5-fold serial dilutions of the cDNA net solutions were used to create a standard curve for each gene. As explained in **section 9.6.2** the Pfaffl relative quantification method requires the crossing point (CP) determination indicated by the threshold (red line) in the normalized fluorescence vs. cycle plot (**panels A** of **Figures 14-21**). The standard curves (**panels B** of **Figures 14-21**) were created by plotting the CP vs. the log concentration of cDNA (ng/µL). The parameters calculated using the standard curve are also indicated **in panels B.** Those parameters were the efficiency (**E**), relative expression rate (**R**) and slope value (**M**). Slope value is required in order to calculate the amplification efficiency [E=10^(-1/slope)] for the Pfaffl equation and should be between the interval of values 3.1<**M**<3.7. The value E, resulted from the standard curve of each gene, is a measure of the overall efficiency of the reaction and should be included in the [0.85; 1.10] interval. R^2 gives a measure of the fitting of the linear regression and the linearity of the PCR assay and the value should be superior to 0.98 inclusive. The assessment of the reaction specificity was also evaluated by melting curve analysis (**panels C** of **Figures 14-21**). The visualization of one single peak indicates a specific amplification of the targeted gene. All plots were created using Corbett software (Corbett Life Science).

IL-1RII mRNA expression level was also analyzed. However, when the PCR amplification of IL-1RII mRNA was performed, to obtain the standard curve, the first two dilutions achieved a Ct value of 40 and the last three dilutions were not amplified. After several attempts, we concluded that this receptor has a very low mRNA expression in our system.

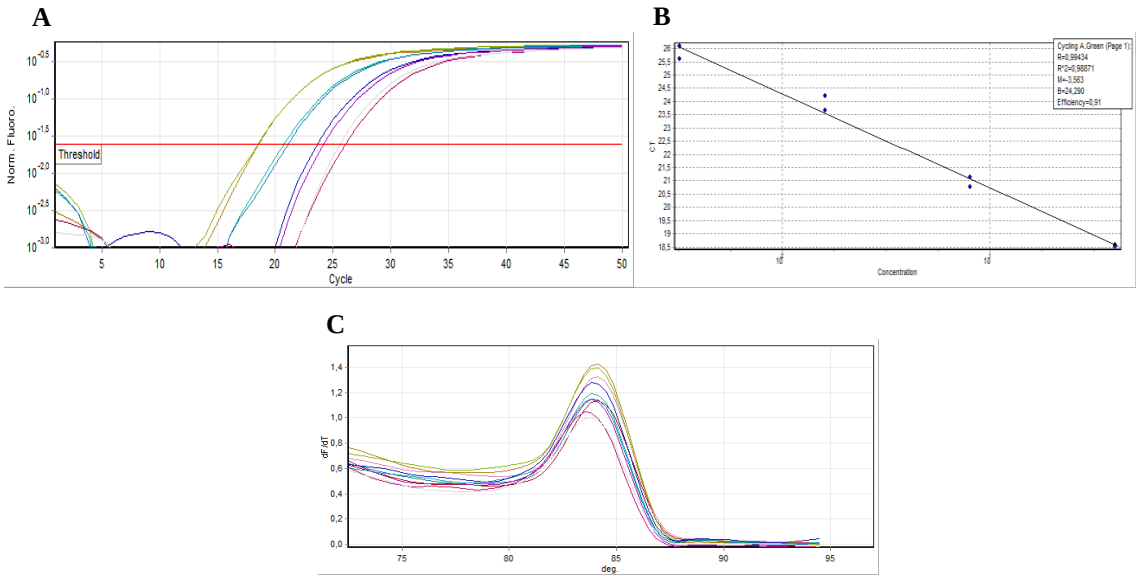

Figure 14 | qPCR Standard and melting curves analysis for the GAPDH gene – endogenous control. A) PCR amplification plot for the GAPDH gene. **B)** Parameters calculated using standard curve created by plotting CP vs. the log concentration of cDNA (ng/µL). **C)** Assessment of reaction specificity by melting curve analysis.

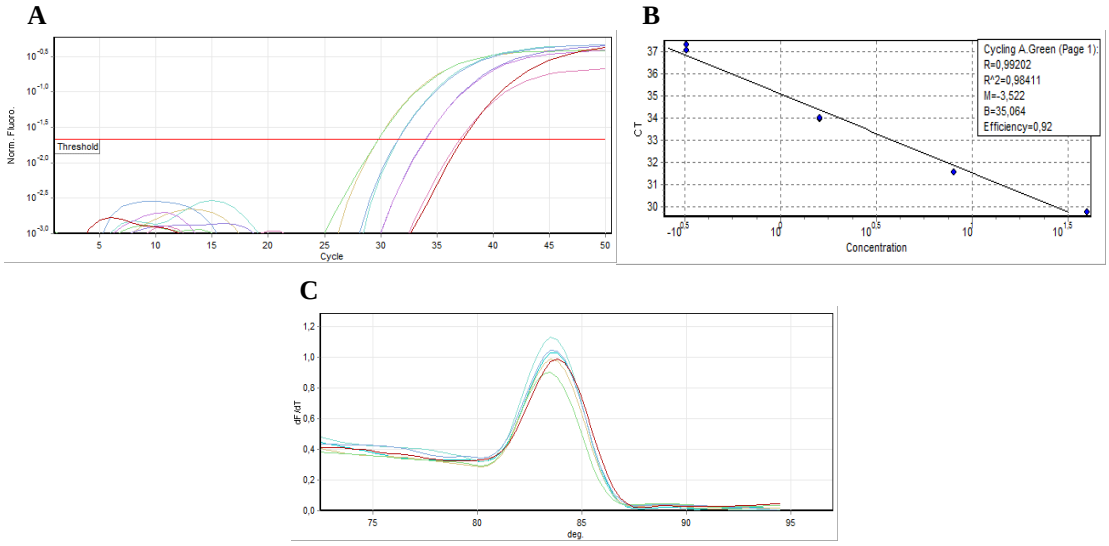

Figure 15 | qPCR Standard and melting curves analysis for the interleukin-1β (IL-1β) gene. A) PCR amplification plot for the IL-1β gene. **B)** Parameters calculated using standard curve created by plotting CP vs. the log concentration of cDNA (ng/µL). **C)** Assessment of reaction specificity by melting curve analysis.

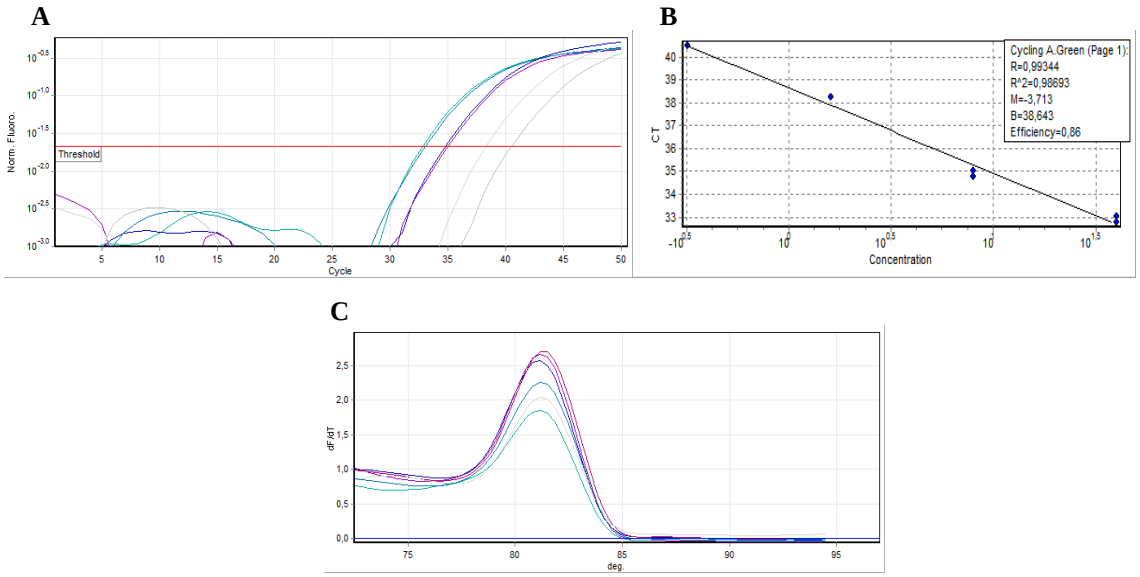

Figure 16 | qPCR Standard and melting curves analysis for the interleukin 1 receptor type I (IL1R1) gene. A) PCR amplification plot for the IL1R1 gene. **B)** Parameters calculated using standard curve created by plotting CP vs. the log concentration of cDNA (ng/µL). **C)** Assessment of reaction specificity by melting curve analysis.

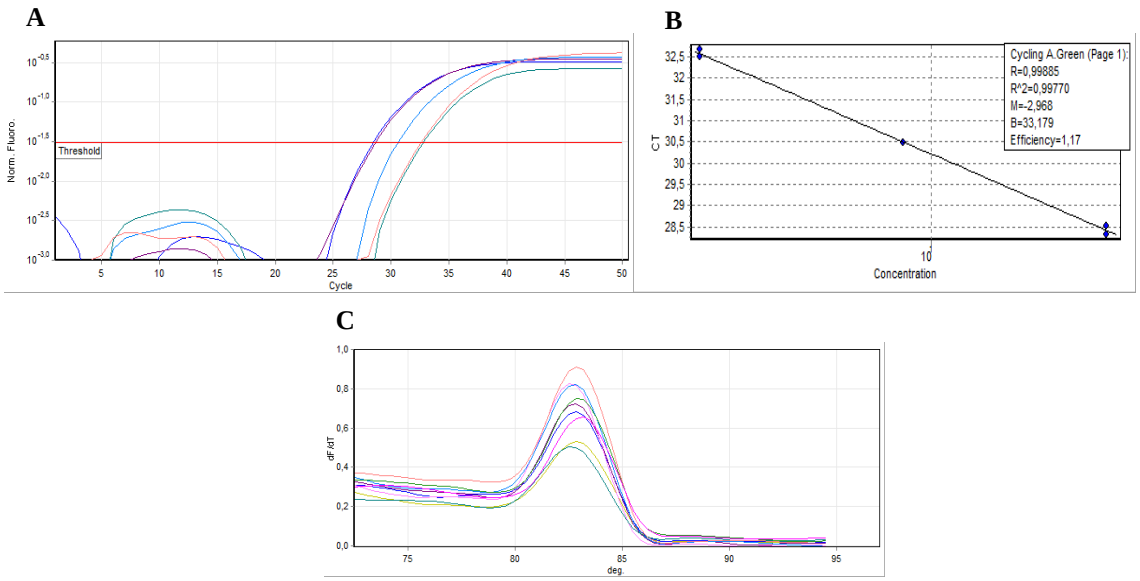

Figure 17 | qPCR Standard and melting curves analysis for the tumor necrosis factor alpha (TNF-α) gene. A) PCR amplification plot for the TNF-α gene. **B)** Parameters calculated using standard curve created by plotting CP vs. the log concentration of cDNA (ng/µL). **C)** Assessment of reaction specificity by melting curve analysis.

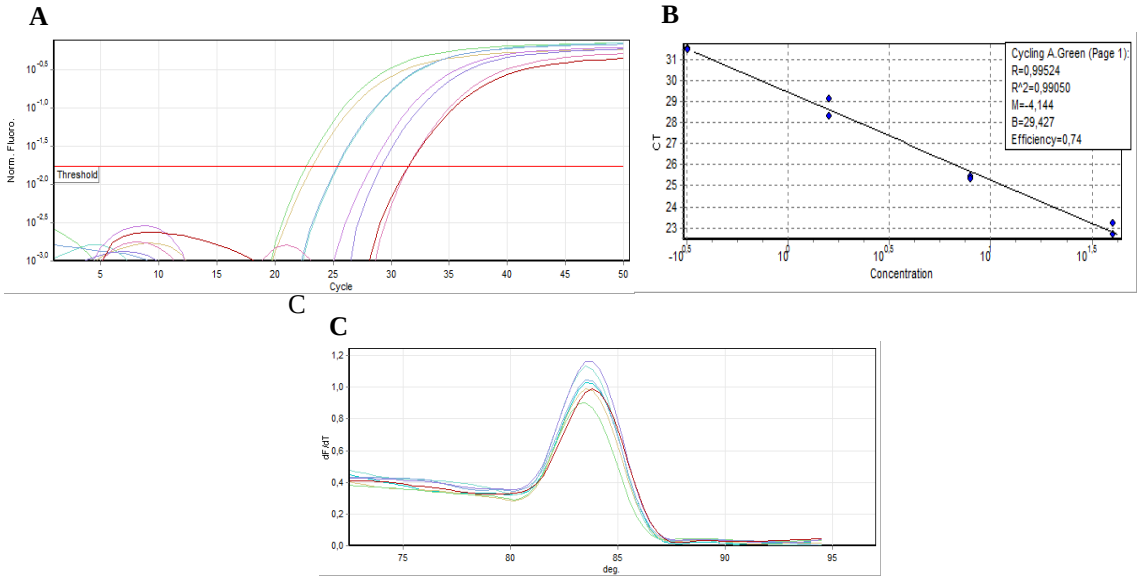

Figure 18 | qPCR Standard and melting curves analysis for the tumor necrosis factor receptor-1 (TNFR1) gene. A) PCR amplification plot for the TNFR1 gene. **B)** Parameters calculated using standard curve created by plotting CP vs. the log concentration of cDNA (ng/µL). **C)** Assessment of reaction specificity by melting curve analysis.

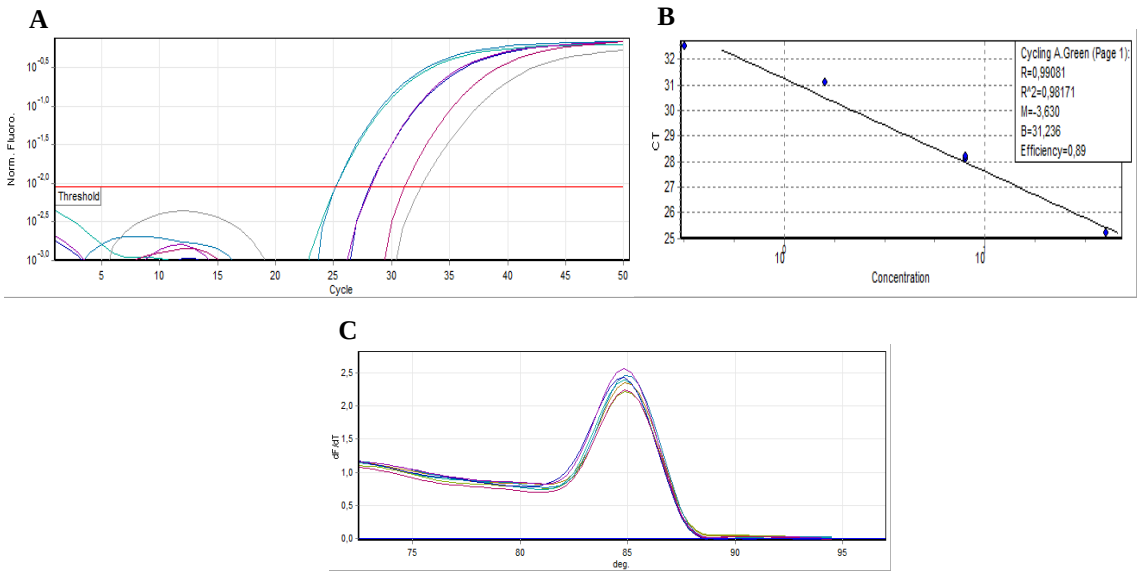

Figure 19 | qPCR Standard and melting curves analysis for the tumor necrosis factor receptor-2 (TNFR2) gene. A) PCR amplification plot for the TNFR2 gene. **B)** Parameters calculated using standard curve created by plotting CP vs. the log concentration of cDNA (ng/µL). **C)** Assessment of reaction specificity by melting curve analysis.

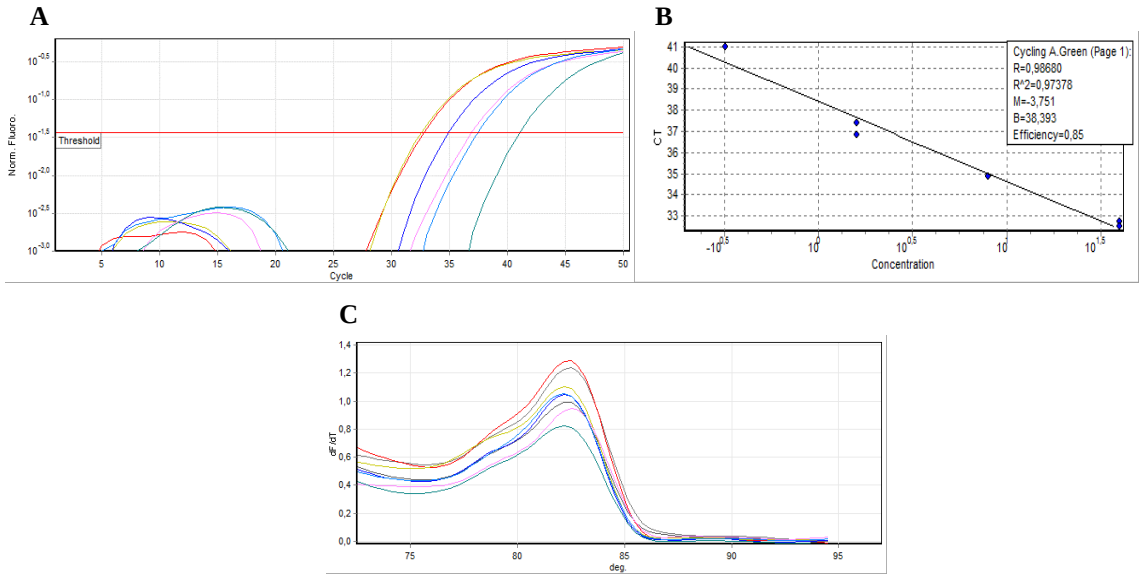

Figure 20 | qPCR Standard and melting curves analysis for the interleukin-6 (IL-6) gene. A) PCR amplification plot for the IL-6 gene. **B)** Parameters calculated using standard curve created by plotting CP vs. the log concentration of cDNA (ng/µL). **C)** Assessment of reaction specificity by melting curve analysis.

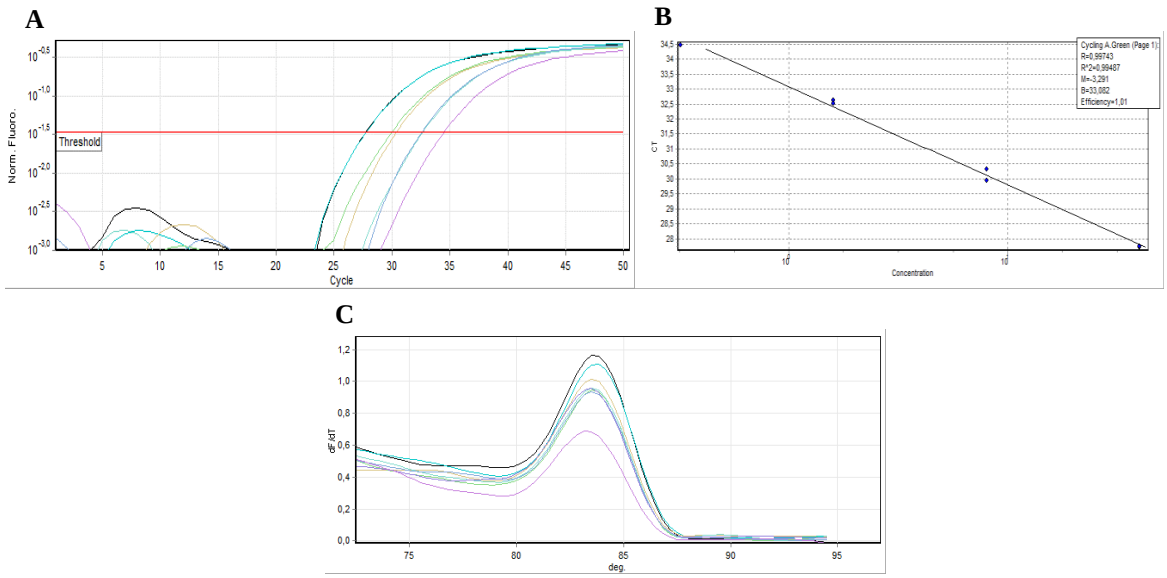

Figure 21 | qPCR Standard and melting curves analysis for the interleukin-6 receptor (IL-6R) gene. A) PCR amplification plot for the IL-6R gene. **B)** Parameters calculated using standard curve created by plotting CP vs. the log concentration of cDNA (ng/µL). **C)** Assessment of reaction specificity by melting curve analysis.

8.8 Agarose gels analysis

Alternatively to the melting curve attained at the end of the run of real-time qPCR, the primers specificity can be analyzed by gel electrophoresis. All real-time qPCR primers must generate a single amplicon of the correct size on agarose gels. As shown in **panels C** of **Figures 14-20** the melting curves of each gene contain a single peak with no shoulders, and the agarose gels (**Figure 21**) also revealed a single band corresponding to the predicted amplicon length of each gene.

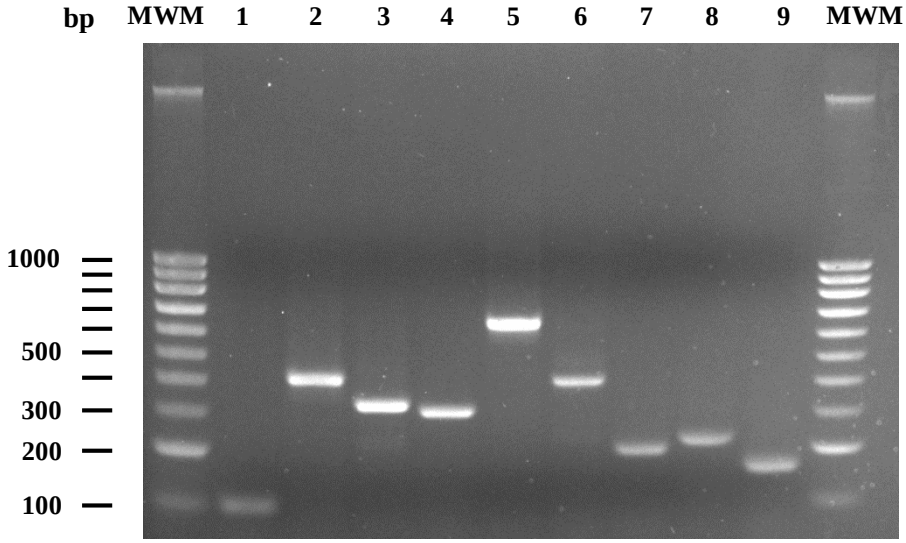

Figure 21 | Gel analysis of the qPCR products. 2% agarose gel shows the PCR product amplified with each pair of specific primers. MWM, molecular weight marker; lane 1 TNFα (106 pb), lane 2, TNFR1 (415 pb), lane 3, TNFR2 (332 pb), lane 4 IL-1β (309 pb), lane 5 IL-1RI (635 pb), lane 6 IL-1RII (336 pb), lane 7 IL-6 (203 pb), lane 8 IL-6R (227 pb), lane 9 GAPDH (170 pb).